EVALUATION OF CONVENTIONAL LCM

TREATMENTS IN FRACTURED AND VUGGY

FORMATIONS

By

GHASSAN DHIYA ALSHUBBAR

Bachelor of Science in Petroleum and Natural Gas

Engineering

West Virginia University

Morgantown, WV

2010

Submitted to the Faculty of the
Graduate College of the
Oklahoma State University
in partial fulfillment of
the requirements for
the Degree of
MASTER OF SCIENCE
December, 2017

EVALUATION OF CONVENTIONAL LCM

TREATMENTS IN FRACTURED AND VUGGY

FORMATIONS

Thesis Approved:

Dr. Runar Nygaard

Thesis Adviser

Dr. Geir Hareland

Dr. Prem Bikkina

Name: Ghassan Dhiya Alshubbar

Date of Degree: DECEMBER, 2017

Title of Study: EVALUATION OF CONVENTIONAL LCM TREATMENTS IN FRACTURED AND VUGGY FORMATIONS.

Major Field: Petroleum Engineering

Abstract: Lost circulation (LC) is an unfavorable event encountered during drilling operations that at extreme situation can jeopardize the whole drilling process. Millions of dollars can be easily accumulated impacting both the economy and the feasibility of such projects. Well control, wellbore stability and stuck pipe incidents are some of the anticipated consequential events caused by lost circulation.

The main objective of this work is to investigate the effectiveness of conventional lost circulation materials (LCM) through 1) studying LCM under a simulated circulation condition (S_{circ}), mimicking wellbore fluid flow, for fractured formations 2) studying losses in vugular formations experimentally and formulate effective LCM recipes.

To address these objectives, a fluid loss apparatus was designed and developed to simulate field conditions (i.e. the overbalance, difference between mud weight and pore pressure, and mimic circulation). Previously reported effective LCM recipes have been retested conventionally, (i.e. no S_{circ}), and under S_{circ} on tapered slotted stainless steel disks (TS), simulating fractured formations. To study losses in vugular formations, stainless steel disks with different irregular opening shapes and sizes were developed. These disks were used first in a low-pressure LCM apparatus (LPA) with different LCM additives to screen out potential effective recipes. The seal integrity of those recipes was then investigated at higher pressure under an overbalance condition using the developed apparatus.

In this research, LCM blends were tested under a S_{circ} replicating more of the actual field behavior in fractured formations. The identified effective LCM blends are expected to have an increased success for field treatments. Also this work is considered as the first attempt to study losses in vugular formations experimentally. The results will significantly enhance the understanding of the seal formation in irregular shape openings.

TABLE OF CONTENTS

Chapter   Page

LIST OF TABLES

LIST OF FIGURES

Figure   Page

CHAPTER I

INTRODUCTION

As conventional reservoirs have been depleted, the oil industry start seeking fields and operational practices that are more challenging. Loss of circulation (LC) is a part of these challenging environments which costs the industry nearly a billion dollars a year (Al Menhali et al., 2014).

LC is defined as losing drilling mud into the formation, named a thief zone, and is classified based on the severity measured in barrels per hour, as 1) Seepage (<10 bbl/hr), 2) partial (10-50 bbl/hr), 3) Severe (>50 bbl/hr), and 4) Total losses (no returns). However, this classification does not explain the loss mechanism resulting in inappropriate treatments. A classification based on root cause was adopted later dividing losses into losses caused by 1) pore throats, 2) induced or natural fractures, and 3) vugs or caverns (Ghalambor et al., 2014).

Losses to pore throat is the least severe and the easiest type of LC events to treat. Bridging theories are used to control this type of LC. These theories were established based on minimizing fluid loss of drill in fluids; to reduce formation damage, through incorporating bridging materials. Abrams (1977) recommended the first criteria to select size and concentration of these bridging materials. Ideal Packing Theory (IPT),a further development to Abrams theory, came to address

and define the full range of particle size distribution (PSD) required to effectively seal all voids (Dick et al., 2000). To achieve minimal fluid loss, Vickers enhanced the IPT and recommended a specific size selection criteria based on D_{25}, D_{50}, D_{75} and D_{90} (Kumar et al., 2010). It would add a value here to mention that Whitfill suggested a similar criterion, called "Halliburton Method", to control fluid loss into fractures. Haliburton Method suggested that D_{50} should be equal to the estimated fracture width (Kumar et al., 2010). Similarly, Alsaba et al. (2016) presented a new criterion to select PSD for an effective fracture sealing. The method was developed based on a comprehensive laboratory investigation of LCM. The criteria suggested D_{50} and D_{90} to be equal or greater than 3/10 and 6/5 the fracture width, respectively.

Induced or natural fractures can be associated with partial to total losses depending on the amount of overbalance (i.e. difference between mud weight and pore pressure) and the width of the fracture (Van Oort and Vargo, 2008). Curing this type of LC is often tied to enhancing the fracture gradient through a number of proposed mechanisms (Fuh et al., 1992; Alberty and McLean, 2004; Dupriest, 2005; Van Oort et al., 2009; Salehi and Nygaard, 2011), a comprehensive summary is presented in Appendix A.

Total loss of circulation is usually linked to vugs which were defined by Nair et al., (2008) as "any pore that is significantly larger than a grain". Vugs can be in centimeter or decimeter scale and are associated with carbonate rocks as a result of the complicated depositional environments and post-depositional diagenesis they experience (Hidajat et al., 2004). Despite the great interest in LC events, only a few studies have been aimed towards curing vugular formations (Savari et al., 2016).

With more understanding of losing mechanisms, researchers started to conduct laboratory studies either to investigate how fracture gradient is being enhanced or to study LCM. With the

former being addressed in Appendix B and outside the scope of this thesis, Chapter II will discuss

and review the LCM laboratory studies in details.

CHAPTER II

LITERATURE STUDY

During the past decades starting from DEA-13 in the 80's, which is considered as the basis of all the fracture gradient enhancement mechanisms, through GPRI in 2000's, (i.e. a project done to revive DEA-13 but in smaller scale), and until our present time; there have been numerous studies focusing on LCM (Van Oort et al., 2009). These studies can be divided into two groups. One group of studies was concerned with identifying effective combinations of LCM that stand a high differential pressure. The other group of studies was more concerned with which physical properties constitutes an effective LCM. In other words, what makes one LCM perform better than the other. A summary of these studies, sorted based on these two groups, is presented below.

EFFECTIVE COMBINATIONS OF LCM

Different testing apparatuses have been designed and used to simulate different aspects of fractured formations with a goal of designing and optimizing effective LCM formulation prior to field application. The following subsections review the findings of these experiments by the apparatus used.

PARTICLE PLUGGING APPARATUS

Particle plugging apparatus (PPA), shown in Figure 2-1, is one of the most common test in evaluating the sealing efficiency of LCM combinations.

Figure II-1 Particle Plugging Apparatus (PPA) (Figure from Kumar and Savari, 2011).

Fractures or porous formations can be tested using slotted stainless steel or ceramic disks respectively. The disks are fitted at the top of the testing cell and thus tested opposed to gravity. The pressure is applied hydraulically from the bottom against a piston that separates the hydraulic and the LCM fluids. Pressure and temperature can be maintained at the desired range while the 30-min fluid loss is being measured. The seal efficiency is measured by increasing the pressure until seal failure.

Kumar and Savari (2011) tested varieties of LCMs and reported ground marble (GM) and resilient graphite (RG) as one of the most effective LCM combination. Further work by Savari et al., (2014) on cellulosic fiber (CF) revealed a significant increase in sealing efficiency when 20% of RG and 0.1-2% of CF are added to the LCM blend.

IMPERMEABLE FRACTURE TEST APPARATUS

For a better fracture simulation which allows for a change in the slot width with the increase in the sealing pressure, the impermeable fracture test apparatus, shown in Figure 2-2 I, was developed by Sanders et al., (2008).
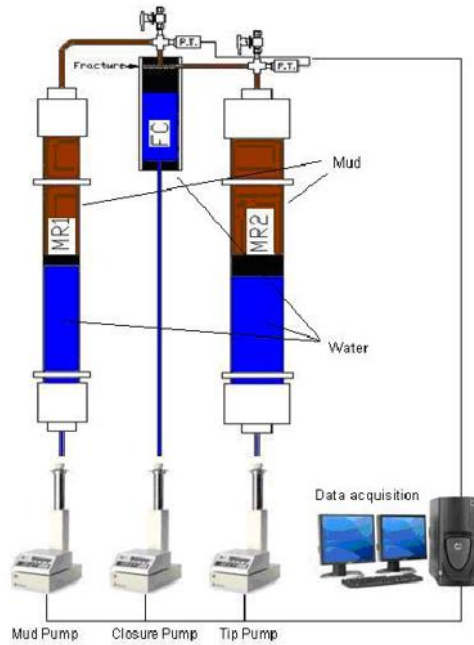
Figure II-2 I) Impermeable Fracture Test Apparatus II) Corrugated Aluminum Plates (Figure from Sanders et al., 2008).

The apparatus consists of three pumps, two accumulators and a fracture cell with two matched uneven aluminum opposed pistons plates, shown in Figure 2-2 II. The minimum fracture width is controlled by three set of screws. The apparatus was designed to be capable of:

- Establishing fracture closure pressure.

- Applying constant pressure at fracture tip.

- Injecting LCM fluid into fracture at a controlled rate.

- Measuring pressure of injected fluid.

- Measuring fracture opening width.

- Measuring volume of fluid lost to fracture tip.

Sanders et al., (2008) evaluated dozens of materials and blends of LCM using this apparatus. This includes, cellulosic, synthetic elastomers, rubber, polyethylene, polypropylene, mica, glass, graphite, petroleum coke-based materials, iron-based compounds and calcium carbonate. Particulates, short & long fibers, platelets, gels flakes, films and irregular/regular spheres were

6

the shapes tested. The most effective LCM formulation was found to involve a blend of various grades of GM, ground nutshell (NS) and graphite /coke. On the other hand, elastomers, rubbers and ground plastics were found to be ineffective.

PERMEABLE FRACTURE TEST APPARATUS

As a further step towards a better understanding of LCM's behavior in permeable formations, a new apparatus "The Permeable Fracture Test Apparatus" was developed by Hettema et al., (2007). Figure 2-3 illustrates a schematic of the apparatus.
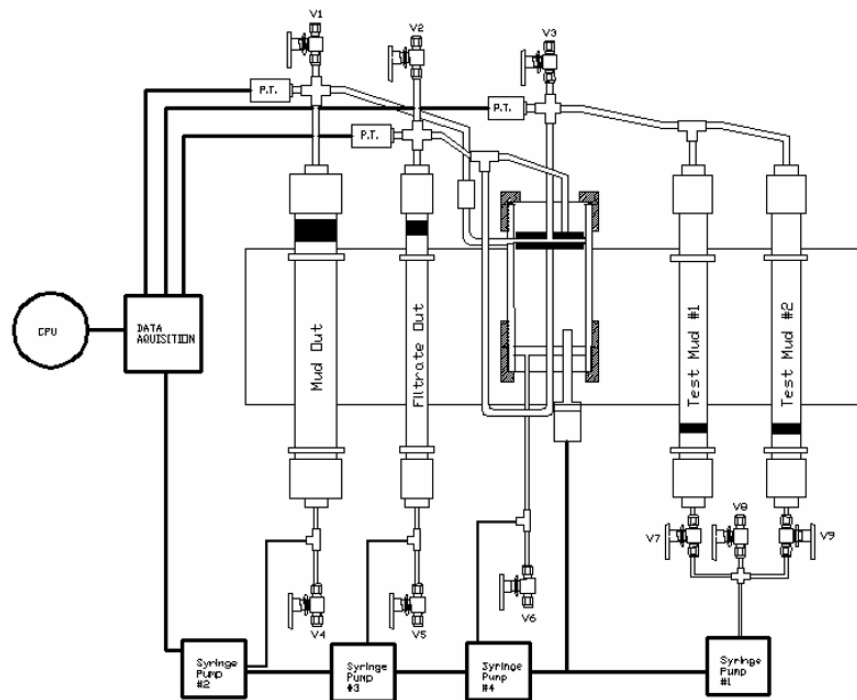
Figure II-3 Permeable Fracture Test Apparatus (Figure from Hettema et al., 2007).

The apparatus consists of 1) four accumulators; to handle pore and test fluid, 2) a cylindrical vessel containing two soapstone plates representing a fracture in a permeable medium, and 3) four syringe pumps. The apparatus was designed to be capable of:

- Measuring fluid losses at the tip & matrix.

- Calculating fracture width.

- Estimating seal location.

Their work reported a moderate correlation of spurt loss volume from the permeably fracture test apparatus with the reported spurt loss volume from PPA tests. The spurt loss volumes were strongly correlated for low loss volumes which also resulted in forming the most efficient seals. The experiment also concluded that a low fluid loss values corresponding to a higher density fluid, more barite, is detrimental to the seal integrity. Thus, an effective seal is obtained through accumulation of sized particles of LCM; not through total solids "barite". Moreover, non-LCM based filtration control additives found to have a positive effect.

LOW AND HIGH PRESSURE LCM TESTING APPARATUSES

The effects of varying LCM type, size and concentration for a range tapered slotted stainless steel disks (TS) were studied using the Low & High Pressure LCM Test Apparatuses developed by Al-saba et al. (2014). The Low-pressure apparatus, shown in Figure 2-4, is a modified version of the API fluid loss tester.
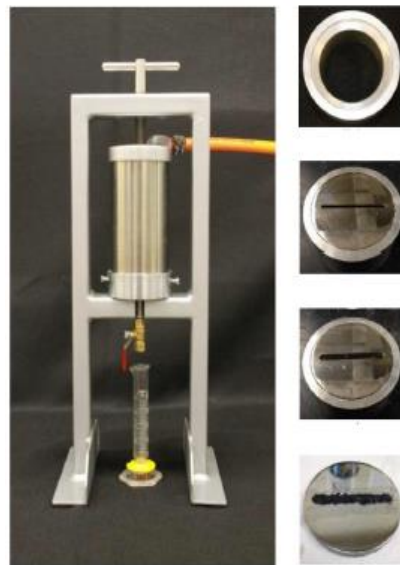
Figure II-4 Low Pressure LCM Test Apparatus (Figure from Al-saba et al., 2014)

It was used to screen out 20 blends of four different LCMs at 15 and 50 pound per barrel (ppb) concentrations. Table 1 shows the formulation of these blends.

LCM Type	D(50) microns	% of Total Concentration if used Individually				% of Total Concentration if used in combinations					
						Graphite & Sized CaCO3		Graphite, CaCO3 & Cellulosic Fiber		Graphite & Nut Shells	
		Case #1	Case #2	Case #3	Case #4	Case #1	Case #2	Case #1	Case #2	Case #1	Case #2
Graphite (G)	50	20	14	0	0	10	6.7	3.6	2.4	10	6.5
	100	20	20	20	0	10	10	3.6	3.6	10	10
	400	30	26	40	50	15	13.3	5.5	4.8	15	13.5
	1000	30	40	40	50	15	20	5.5	7.3	15	20
Sized CaCO3 (SCC)	5	16	6	0	0	3	0	4.4	0	--	--
	25	16	6	0	0	3	0	4.4	0	--	--
	50	16	13	0	0	7	0	9.5	0	--	--
	400	16	21	33	20	11	16.5	15.3	24	--	--
	600	18	27	33	27	14	16.5	19.6	24	--	--
	1200	18	27	34	53	14	17	19.6	24.7	--	--
Nut Shells (NS)	620	33.3	0	0	0	--	--	--	--	16.5	16.5
	1450	33.3	50	100	0	--	--	--	--	16.5	16.5
	2300	33.3	50	0	100	--	--	--	--	17	17
Cellulosic Fiber (CF)	312	50	100	0		--	--	4.5	4.5	--	--
	1060	50	0	100		--	--	4.5	4.5	--	--

Table 1: LCM Blends reported in Al-Saba et al., 2014.

Out of 160 tests conducted with four different fracture sizes, only 26 blends were successful. These blends were then evaluated for their sealing efficiency using a High Pressure LCM Test Apparatus, shown in Figure 2-5.
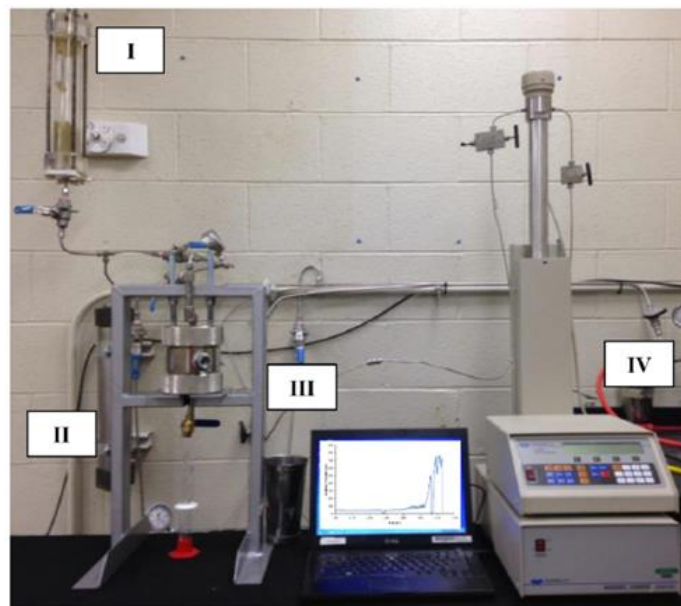
Figure II-5 High Pressure LCM Test Apparatus (Al-Saba et al., 2014)

This experimental setup was designed and constructed with I) a plastic accumulator, II) metal accumulator, III) testing cell containing LCM Fluid and tapered disks, and IV) a syringe pump.

The testing cell can be heated up to 300˚F using an insulated heating blanket. The conclusion drawn based on this experiment was as follow:

- Fibrous materials showed superior performance due to the wide range of PSD, the irregularity in particles shapes and their deformability.
- Optimizing PSD is the key for successful treatment.
- Granular materials (GM, RG) have lower seal integrity.
- Higher concentration of LCM yields higher sealing pressure.
- A strong relationship between Fluid loss and sealing efficiency is observed.
- At high temperature, NS had 54% increase in sealing efficiency due to swelling.
- No aging effect on RG and GM.
- The effect of temperature on fluid loss is not significant.

EFFECTIVE LCM PROPERTIES

Several approaches and different experimental setups were used to identify the required physical characteristics of effective LCM treatments. LCM properties including mechanical properties, size, shape, strength and texture were studied. This section reviews the findings of these studies.

Sanders et al., (2008) listed the essential LCM properties needed to formulate a successful treatment through studying effective LCM recipes experimentally. These properties are as below:

- **Particle Size and Size Distribution:** The maximum size required should be determined by the anticipated fracture width with a good PSD to ensure optimal bridging.
- **Particle shape and Texture:** Spheroidal-shaped particles with rough surface and low aspect ratio are the optimum shape to maximize the sealing pressure.

- **Particle Concentration and Bulk Density:** For API barite-weighted fluids, 20 ppb is a typical minimum concentration. Low specific gravity material has an advantage as more particles are present for a given weight.

- **Particle Compressive Strength (CS):** Materials with high CS exhibits a more efficient seal.

- **Resiliency:** High resilient materials play an important role in forming effective seal.

To identify the ideal LCM shape (i.e. The aspect ratio, sphericity and convexity), optical microscope imager examination was conducted on a variety of LCMs. The effective LCMs were found to have similar shape factor values. Table 2 presents the shape factor of different effective LCMs studied by Kumar et al., (2010).

Product	Generic Name	Nominal Diameter (μm)	Aspect Ratio	Sphericity	Convexity
GM 150	Ground Marble	150	1.42	0.54	0.96
GM 600	Ground Marble	600	1.57	0.51	0.96
RGC 400	Resilient graphite Carbon	400	1.57	0.46	0.90
RGC 1000	Resilient graphite Carbon	1000	1.42	0.53	0.91
Ground Nutshells M	Ground Nut Shells	1450	1.50	0.50	0.91
Ground Nutshells F	Ground Nut Shells	617	1.37	0.55	0.92
Ground Rubber	Ground rubber	300	1.39	0.53	0.88
Cellulosic Fibre	Wood fibre	1063	1.63	0.44	0.92

Table 2 Shape Factor of Different LCM (Kumar et al., 2010).

The importance of the compressive strength and the resiliency of effective LCM treatments are perceived through the understanding of fracture behavior during drilling operation. As the bottom hole pressure fluctuates, due to the equivalent circulating density (i.e. the added pressure due to frictional losses in the wellbore), a cycle of fracture opening and closing occurs, shown in Figure 2-6, which results in compression forces that stress the LCM seal.

(a) ECD>FCS   (b) FCS>ECD   (c) ECD>FCS
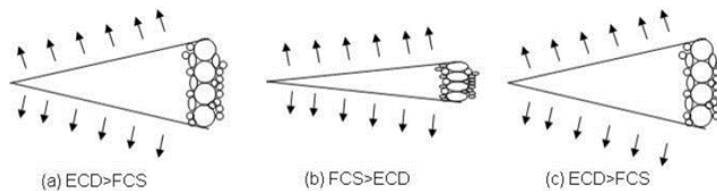
Figure II-6 ECD & Fracture Width (Figure from Kumar et al., 2010).

According to Kumar et al., 2010, to maintain a seal the LCM needs to have some level of crushing resistance and resiliency enabling it to stand the compression forces and rebound to fill the space as the fracture reopens. Tinius Olsen hydraulic tester (TO) was used along with other apparatuses to study these properties and following conclusions were drawn:

- GM acts as a brittle material, reduction in particle size under load, with zero resiliency.
- NS acts as a ductile material, increase in particle size under load, with approximately 16% resiliency.
- RG exhibits minor changes in size and resiliency of 120%
- Addition of just 20% by Volume of RG can significantly increase the crushing resistance of LCM and inhibits significant resiliency to a LCM blend.

A different perspective based on granular-matter mechanics was pursued by Xu et al., (2014) to identify the required properties of effective LCMs. The study examines the structural and mechanical properties of the formed seal as a whole. The LCM seal was found to be intrinsically multiscale; micro, meso and macro. The single particle represents microscopic scale while the seal represents the macroscopic scale. The mesoscopic scale was defined by a chain force developed by several particles constantly contacting each other under external load. Figure 2-7 illustrates this concept.
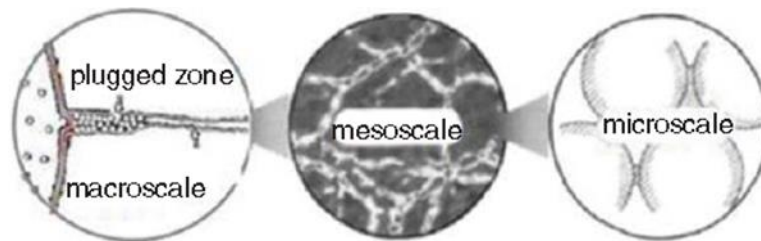
Figure II-7 Multiscale Framework (Figure from Xu et al., 2014)

This chain force was suggested to support most of the crushing and shearing stresses thus directly effecting the integrity of the formed seal. The following factors were set to be the basis upon which effective LCM needs to be formulated.

- **Contact deformation:** a high value of elastic contact deformation strongly affects the strength of the force chain. Thus, the addition of deformable material such as RG increases the stability of the seal. 10 -20% by volume usually gives an acceptable contact deformation and would not adversely affect the strength of the seal.

- **LCM volume fraction:** it reflects the compactness of the seal, and will directly affect the stability of the chain force. Fiber materials have smaller diameters compared to other particles and can fill in the pores in between. Therefore, the efficiency of the seal will increase by the addition of fiber. The minimal recommended length of the fiber is twice the circumference of the largest particle. Moreover, the ratio of the length of the fiber to its diameter is constrained by the equation below:

$$\frac{L_f}{D_f} \leq \frac{\sigma_{fu}}{2\tau} \quad (1)$$

σfu: yield strength of fiber, τ: average shear stress

- **Surface friction coefficient:** Surface friction coefficient is in direct relationship with the shear resistance a force chain possesses. Thus, a particle with small diameter, low sphericity and convexity would result in a higher surface friction coefficient yielding into higher sealing pressure seal.

Based on the information presented above, a blend of rigid granules, fiber and resilient particles believed to produce the most efficient seal. Hence, GM, CF and RG were used in a set of experiments to determine reliability of this study. Figure 2-8 illustrates the seal efficiency at different combinations and concentrations of these LCM:
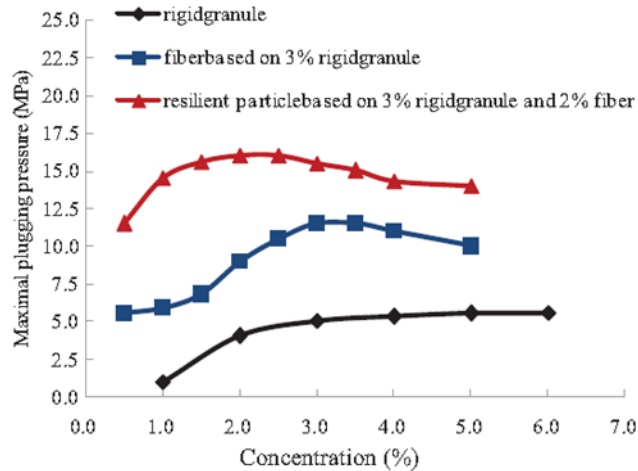
Figure II-8 Blend seal efficiency (Figure from Xu et al., 2014)

CRITICAL REVIEW

The experiments and apparatuses discussed earlier were aimed to either identify effective LCM formulations or study the properties of effective LCMs themselves. In identifying effective LCM formulation, the laboratory testing meant to mimic real-life environment and down hole conditions, such as permeability, temperature, pressure and fracture width & shape. However, there are some limitations and shortcomings associated with each set up such as pressure, LCM size, and some settling concerns. This section will highlight the deficiencies for each laboratory setup aiding in identifying current gaps and potential research emphasis.

For the PPA, the floating piston inside the pressure cell imposes a reliability concerns as LCM may settle at the piston surface and pushed at higher concentration through the slotted disk. Also, the action of the fluid carrying the LCM inside a wellbore and through the fracture is not properly simulated. These two limitations may result in inaccurate seal efficiency determination.

14

The concern with the permeable and impermeable fracture test apparatuses is the limited sizes

of LCM particles that can be used. The LCMs were limited to only 1000 microns, to avoid tube

plugging, resulting in a restriction in fracture size simulation.

The high-pressure LCM testing apparatus was associated with LCM settling, as testing

conducted with the gravity, and resulted screen outs of thick plugs at TS surfaces, Figure 2-9. The

thick plug may provide a temporary static seal and once drilling operations are resumed the seal

integrity may be jeopardized as a result of the fluid movement along the wellbore.
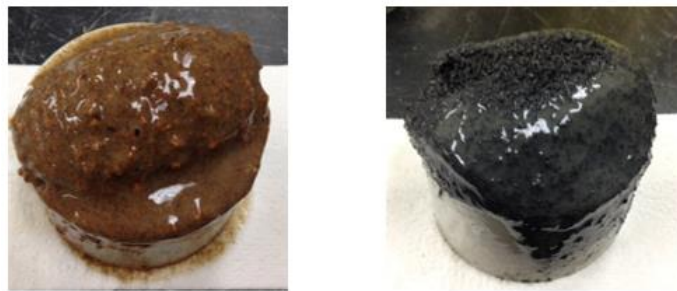
Figure II-9 Thick Plugs Screened Outs (Al-Saba et al., 2014)

Since the reported essential LCM properties (i.e. size, compressive strength, particle shape and

texture, and resiliency) were based on studying effective LCM recipes, any shortcomings or

limitation in laboratory setups during formulating stage could be carried on; resulting in

erroneous conclusion. Thus, limitations in current apparatuses should be addressed first, to

confirm the effectiveness of the LCM formulation, prior to conducting any studies on LCM

physical properties. However, this is outside the scope of this work and will not be investigated

any further.

CHAPTER III

RESEARCH OBJECTIVES

The critical literature review in Chapter II revealed some limitations and concerns with the used apparatuses. Despite the efforts to overcome these limitations, by developing better devices, shortcomings were still associated with each set up. LCM size limitation, LCM settling concerns with the downward flow, and piston forcing the LCM into the slot are all issues that needed to be addressed. Moreover, the effect of fluid movement along the wellbore, during circulation, on the seal integrity of LCM has not been considered. It is hypothesized that the crossflow along the fracture caused by the circulation of drilling fluid during drilling operations is reducing the LCMs ability to enter the fracture. On the other hand, almost all experiments were aimed to seal induced/ natural fractures only. Experimental work to cure losses to vugular formation was rare. The main objectives of this work are to 1) study the effects of circulation and mud movements on LCM seal integrity for fractured formations 2) study losses in vugular formations experimentally and formulate effective LCM recipes. To achieve these objectives, the subsequent steps were followed:

1. Develop a fluid loss apparatus that is capable of simulating circulation and overbalance conditions.

2. Evaluate effective LCM recipes under simulated circulation condition (Scirc) and study any sealing deviation for fractured formations.

3. Characterize vugs in dolomites by investigating analogs.

4. Develop stainless-steel disks that mimic vuggy formation.

5. Formulate LCM recipes for vuggy formation using Low Pressure LCM apparatus.

6. Evaluate the integrity of the formulated vugular LCM recipes under simulated field condition, overbalance, at high pressure.

The completion of the steps above resulted in a better understanding of the effect of S_{circ} on the formation and integrity of LCM seal in fractured formations. Also enhance our understating of seal development in vuggy formations.

CHAPTER IV

METHODOLOGY

This chapter discusses in details the steps and processes used to achieve the research goals outlined in Chapter III. It includes the designing and the fabrication of the dynamic fluid loss apparatus, testing setups and methodologies, fluid formulation, and the development of vuggy disks.

DYNAMIC FLUID LOSS APPARATUS AND EXPERIMENT SETUPS

To introduce a simulated circulation condition (S_{circ}), a crossflow along the fracture and evaluate LCM at high pressure, a commercially available stirred fluid loss tester (M7150 Stirred Fluid Loss Tester User Manual, 2017) has been chosen as a base of the build due to the similarity in the functions needed. This apparatus has the ability to pre-condition slurries, simulating down hole environment, and test for fluid loss statically on either a filter mesh or a filter paper. A rotating shaft is connected to a paddle assembly which stirs the slurry at 150 rpm, shown in Figure 4-1. Temperature can be varied from 0°F to 400 °F. Once the slurry is pre-conditioned, the shaft is disconnected and the cell is set upside down. Pressure and back pressure can then be applied with nitrogen gas and the fluid loss is collected at the bottom.
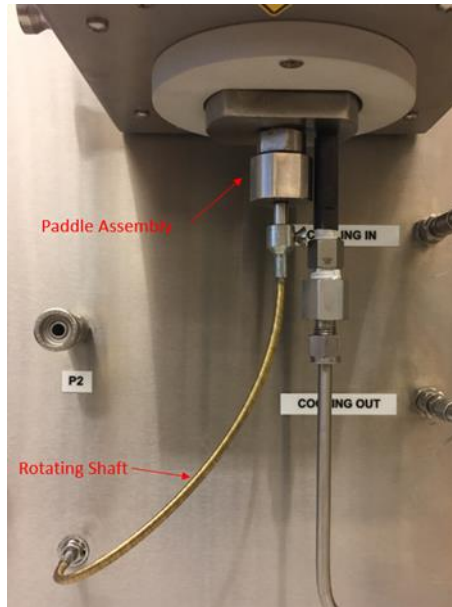
Figure IV-1 Rotating Shaft

Several changes were made on the tester to prepare for LCM S_{circ} testing. A new cell was fabricated to handle LCM mud, fit the tapered slotted disks, and ensure a thoroughly mixing of the LCM mud by positioning the disks closer to the paddle tip, Figure 4-2.

Figure IV-2 I. Factory Testing Cell II. New Fabricated Testing Cell

The simultaneous stirring action and fluid injection along with fluid loss and seal integrity measurements were accomplished by incorporating the modified fluid loss cell (Figure 4-2) and build a flow apparatus, The Dynamic Fluid Loss and Seal Efficiency Tester (DFL&SET) shown in Figure 4-3.
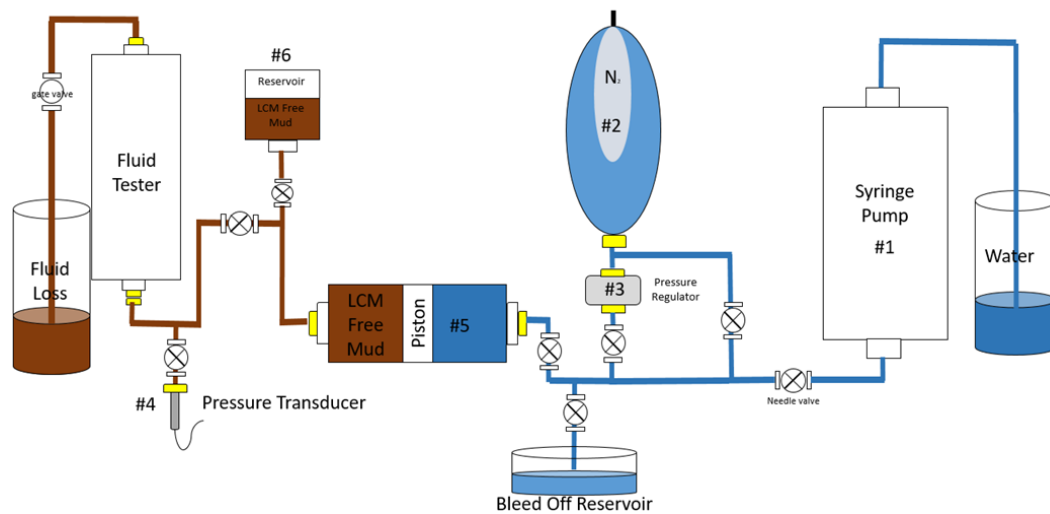
Figure IV-3 The Dynamic Fluid Loss & Seal Efficiency Tester (DFL&SET)

In this setup, drilling mud was used instead of nitrogen gas as an injection fluid. This option mitigated any concerns of gas migration as pumping is performed against the gravity. The tester is designed to provide either constant flow or constant pressure, 0-1000 psi, modes achieved by 1) syringe pump and a 2) bladder accumulator combined with 3) pressure regulator respectively. The pressure is recorded electronically at two points, the syringe pump and 4) a pressure transducer. The pump and the regulator are protected from any corrosive fluid and any plugging concerns are avoided by using 5) a floating piston accumulator. The accumulator provides the means of separating the two fluid, mud & distilled water, and transferring the pressure. 6) A plastic accumulator is used as a mud refilling reservoir if needed.

FORMULATION OF DYNAMIC TESTING FLUIDS

Formulating drilling fluid with an accepted carrying capacity, to prevent LCM settling, under the S_{circ} was a challenge. Since most drilling fluids are non-Newtonian, their viscosity and carrying capacity decreases with the increase in shear rate. According to Baldino et al., (2015) "At medium and high shear rates the dynamic viscosity of drilling fluids decreases considerably and the effect of yield stress is no longer present". Moreover, the work done by Murphy et al., (2006) indicated that under dynamic condition gel strength can't build fast enough to support

particle suspension. The other downside of stirring action observed was getting LCM pushed towards the wall of the cell causing them to settle much quicker than the one in the center; which is in correspondence to observations by Fang (1992).

To overcome these problems Hydroxyethyl Cellulose (HEC) was added to 7% by WT bentonite mud, Mud 1. The HEC contributed towards adding more pseduoplasticity to the fluid. According to Powell et al., (1991), pseudoplastic fluids exhibits higher velocity gradient in the center of the flow stream with more viscous stagnant fluid at the wall. HEC also exhibits higher shear stress with the increase in shear rate. The combination of both characteristics of HEC dramatically improved settling issues. A 15.4 ppg barite weighted bentonite mud, Mud 2, was also found to be effective at S_{circ}. The increase in mud weight gave an improved carrying capacity of the fluid with zero settling rate at static condition. Table 3 illustrates the formulations and rheology of both muds.

Components	Mud 1	Mud 2
Water	100 cc	100 cc
Bentonite	7.6 g	7.6 g
HEC	0.54 g	0 g
Barite	0 g	161 g
WT	8.7 ppg	15.4 ppg
$\theta 3$	55	48
$\theta 6$	57	51
$\theta 100$	82	72
$\theta 200$	93	89
$\theta 300$	104	104
$\theta 600$	128	146
PV	24	42
Yield P	80	62

Table 3 Mud Formulation & Rheology

To test the carrying capacity of both mud formulations under the S_{circ}, a fixed volume of mud was collected repeatedly starting at the bottom of the cell after 20 min of stirring. The LCM were screened out from the mud and weighted up. Table 4 shows the percentage of particle distribution along the height of cell.

	LCM Recipe	
Position	NS & G	G & SCC # 2
	Mud 1	Mud 2
Bottom	24%	27%
	16%	17%
	13%	20%
	20%	15%
	12%	10%
Top	14%	11%
Total	100%	100%

Table 4 LCM Distribution along the Cell Height

Table 4 indicates that the 7 wt% HEC (Mud 1 Table 3) or weighted mud (Mud 2 Table 3) prevents settling for the duration of the testing and those two mud formulations was used for the study. The procedure for all tests was to fill the cell with LCM mud to the tip of paddle, while the space above the paddle and towards the cell end cap was filled up with normal mud to ensure adequate stirring of LCM and prevent sealing before flow was initiated.

TESTING METHODOLOGY FOR FRACTURED FORMATION EXPERIMENT

In this set of experiments, effective LCM formulations with proper concentration and particle size distribution (PSD), to seal a given fracture width, have been chosen from a previous reported study (Al-saba et al., 2014). The formulations consist of graphite (G), size calcium carbonate (SCC), Nutshell (NS) and cellulosic fiber (CF). Table 5 illustrate the formulations and PSD.

LCM Type	D(50) Microns	LCM Blend			
		G & NS	G & SCC (1)	G & SCC (2)	G,SCC, & CF
		% of total concentration			
Graphite (G)	50	10	--	--	3.6
	100	10	--	--	3.6
	400	15	--	--	5.5
	1000	15	--	--	5.5
Sized Calcium Carbonate	5	--	--	--	4.4
	25	--	--	--	4.4
	50	--	--	--	9.5
	400	--	--	--	15.3
	600	--	--	--	19.6
	1200	--	--	--	19.6
	1400	--	33	33	--
	2400	--	--	33	--
Nut shell	620	16.5	--	--	--
	1450	16.5	--	--	--
	2300	17	--	--	--
G & SCC Blend	500	--	67	34	--
Cellulosic Fiber	312	--	--	--	4.5
	1060	--	--	--	4.5
Particle Size Distribution	D10	180	90	170	55
	D25	400	400	650	10
	D50	1000	700	1300	450
	D75	1600	1200	1900	850
	D90	2000	1400	2600	1200

Table 5 Effective LCM Recipes & PSD

The study used two sizes of tapered stainless steel disks, TS1 and TS4, which manufactured locally in accordance to Al-saba et al. (2014) disks' specifications. The two disks have dimensions of 2.5" in diameter and 0.25" in thickness. The opening widths of fracture mouth and tip of TS1 disk were 2500 and 1000 microns respectively while they were 5000 and 2000 microns for the larger disk (TS4).

The LCM formulations were re-tested under conventionally, no S_{circ}, at 25 ml/min flowrate to assure their viability, as they are tested opposed to gravity, and to obtain a reference point for proceeding S_{circ} testing. The effectiveness of these LCM recipes was then studied under a S_{circ} at various flowrates ranging from 10 ml/min to 175 ml/min. The changing in flowrates has magnified and highlighted the effect of the S_{circ} on the LCM treatments. Appendix B details the testing procuders.

DEVELOPMENT OF VUGGY DISKS

To characterize vugs in dolomites, analog formations of dolomitic sediment were investigated.
Thin sections of Thornton outcrop dolomite core, shown in Figure 4-4. a, were found to have 3
mm to 14 mm irregular shape opening networks (Zakaria et al., 2012). Similar vuggy networks
but with only 1 mm to 5 mm opening sizes were identified while studying West Texas field
carbonate cores (Hidajat et al., 2004). The Miami oolite and the Niagaran Michigan pinnacle reef
carbonate cores, presented in Figure 4-4. b, observed to have opening sizes reaching as large as
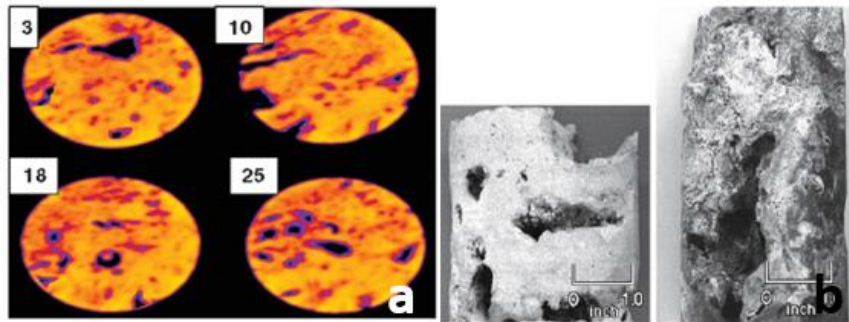20 mm (Lucia, 2007).

Figure IV-4 a.Thin Section of Vuggy Core (Zakaria et al., 2012) b. Vuggy Carbonate Cores (Lucia, 2007).

Stainless steel disks with irregular shape openings were designed and developed to mimic the
shape, the size and the distribution of vugs in the offshore Khuff formation (For further
description see Al-Shubbar and Nygaard, 2018). As a size criterion, an equivalent vug diameter
(EVD) was introduced and defined as the maximum width along the longest vug axis. With the
variety of vug opening sizes, four stainless steel disks, shown in Figure 4-5, were manufactured
with 5 mm, 7.5 mm, 10 mm and 12.5 mm EVDs. These disks were 2.5” in diameter and 0.25” in
thickness.

Figure IV-5 Stainless Steel Vuggy Disks

LCM AND FLUID FORMULATIONS FOR VUGGY FORMATION EXPERIMENT

To formulate a successful LCM treatment, certain key criteria needs to be satisfied (Sanders et al., 2008; Kumar et al., 2010, Al-Saba). Particle size & size distribution are one of these key elements upon which LCMs were screened and chosen. Based on Vickers et al., (2006) bridging theory, only a limited number of commercially available LCM have met the upper portion of the needed PSD; due to vugs unusual large openings. These products were ground wood (GW), synthetic fibers (SF), and highly compressible and resilient reticulated foam materials (FM). Other noncommercial products, synthetic rubbers (SR) and calcium carbonates (SCC), were specifically manufactured and sized to requirement. For field practicality, the maximum particle size was limited to 12,500 microns, with an exception for FM due to its high compressibility. This upper size limit enables the use of downhole multiple activation bypass systems (circulation subs) and eliminates the need of using open ended drill pipe. Other surface restriction, such as mud pump, was not investigated. Smaller size commercial LCM products such as nutshell (NS), graphite (G), and acid soluble fibers (ASF) were used in the formulations to maintain proper PSD and effectively initiate impermeable seals.

The testing fluids used in the experiments were simple 7% bentonite water-based muds (WBM). The simplicity of the mud eliminates any negative or positive effects, if any, of drilling fluid additives such as fluid loss reducers or viscosifiers on LCM performance. Unweighted WBM, Mud 1, was used in the majority of the testing while a 15.4 ppg barite weighted bentonite

mud, Mud 2, was used in SCC LCM formulations to prevent any settling issues. Table 6 illustrates the formulations and rheology of both drilling fluids.

Components	Mud 1	Mud 2
Water	100 cc	100 cc
Bentonite	7.6 g	7.6 g
Barite	0 g	161 g
WT	8.7 ppg	15.4 ppg
PV	10	42
Yield P	19	62

Table 6 Mud Formulation and Rheology

TESTING METHODOLOGY FOR VUGGY FORMATION EXPERIMENTS

Several combinations of LCM were mixed at different concentrations with the proper PSD. These blends were evaluated by the low-pressure LCM apparatus (LPA) that was locally manufactured based on the standard API filter press design. The LPA served as a quick indicative measurement of whether a seal would form with the used LCM's combination, concentration and PSD. The test starts by filling the cell with mud containing the LCM mixture and then applying a pressure of 125 psi to force the LCM fluid to flow through the vuggy disk. If a seal is formed, the LCM mixture is considered for further evaluation at higher pressure using the DFL&SET, Figure 4-4.

In the DFL&SET, the cell is filled by the potential LCM formulation and tested in constant pressure mode. The cell is pre-pressured to 300 psi, to simulate the overbalance condition, prior to allowing fluid to flow through the vuggy disk against the gravity. If seal is formed, the seal integrity is then tested in constant flow mode at 25 ml/min until seal failure and maximum pressure is recorded. Appendix B details the testing procuders.

RESULTS AND DISCUSSION

FRACTURE DISKS RESULTS

The study was conducted, as per the test procedure and methodology presented in chapter 4 to qualitatively determine the effect of the S_{circ} on the different tested LCM blends. The results are presented below in Table 7.

LCM Blend	G & NS		G & SCC(1)		G,SCC, & CF		G & NS		G & SCC(2)	
Total Concn. (ppb)	20		105		55		40		105	
Mud Type	Mud 1								Mud 2	
Disc #	TS1								TS4	
Testing condition	$V_{initial}$ (ml)	P_{max} (psi)	$V_{initial}$ (ml)	P_{max} (psi)	$V_{initial}$ (ml)	P_{max} (psi)	$V_{initial}$ (ml)	P_{max} (psi)	$V_{initial}$ (ml)	P_{max} (psi)
Conventional at Q=25	39 / 32	3000+ / 3000+	22 / 27	2933 / 3000	73 / 82	1211 / 1598	149	1310	53	3000+
S_{circ} at Q=10	294 / 307	528 / 464	--		--		--		--	
S_{circ} at Q=25	255 / 259	1382 / 1621	No Seal		135 / 140	441 / 536	No Seal		No Seal	
S_{circ} at Q=50	67 / 74	2993 / 2957	--		85 / 100	666 / 676	--		No Seal	
S_{circ} at Q=75	62 / 52	3000+ / 3000+	109 / 93	1280 / 945	67 / 79	961 / 983	198	271	No Seal	
S_{circ} at Q=100	--		--		--		--		195	3000+
S_{circ} at Q=125	--		98 / 80	2001 / 1817	--		186	860	116	3000+
S_{circ} at Q=175	--		62 / 76	1882 / 1901	--		--		--	

Table 7 Testing Matrix and Results

In Table 4, $V_{initial}$ represents the initial volume at which the first seal was developed. While P_{max} represent the highest seal pressure recorded. Moreover, each individual test for TS1 was repeated several times to insure the reliability of the results.

For a better data illustration, the results from Table 7 are plotted and presented below in Figure 5-1.
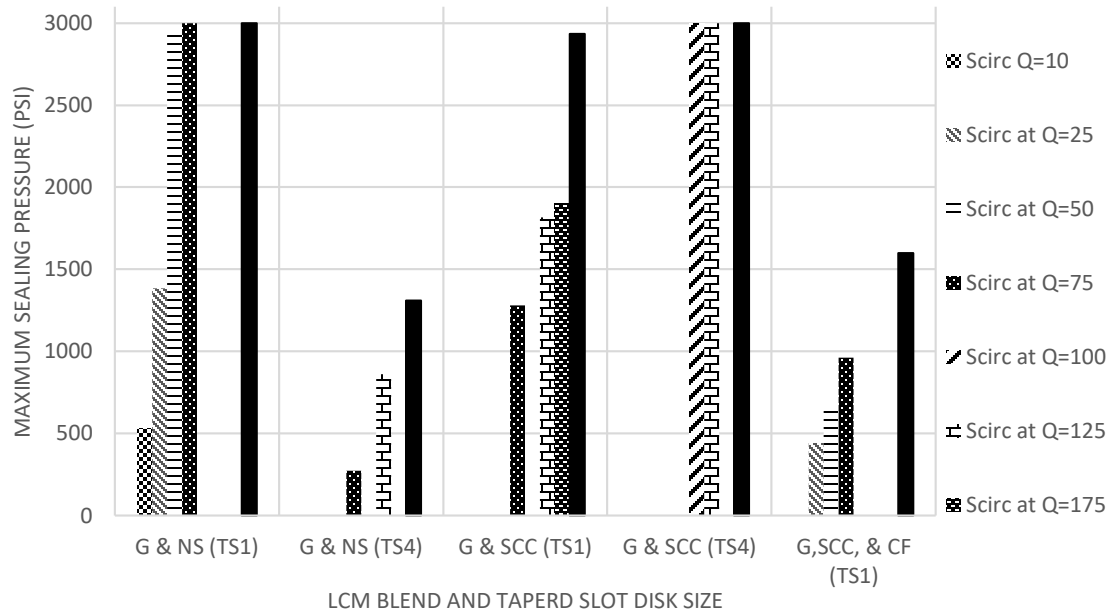

Figure V-1 Effect of Flowrate and Testing condition on Sealing Pressure for the used LCM Blends

The figure shows a relationship between sealing pressure and flowrate for the S_{circ} for the used LCM blends; with the exception of G & SCC (TS4). Some LCM blends at high flowrate exhibit similar sealing pressure as at conventional condition while others lost about 35% of their strength. The below subsections, sorted based on LCM blends, explain these observations and discuss the data in detail.

GRAPHITE AND NUTSHELL

For the tapered and slotted disk, TS1, G & NS LCM formulation was mixed in Mud 1 and tested conventionally at a flowrate of 25 ml/min under S_{circ} at flowrates of 10, 25, 50 and 75 ml/min respectively. The results of each test was plotted as Pressure Vs. Time to facilitate a better

visualization of the data and enable for further analysis. For static testing, two runs were performed and plotted below, Figure 5-2:
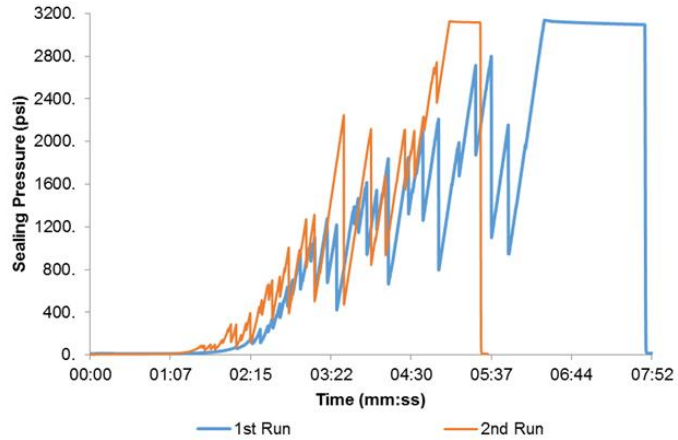

Figure V-2 Conventional Testing of 20 ppg NS & G TS1 @ 25 ml/min

The figure shows with conventional testing condition the seal the seal starts to initiates ($V_{initial}$) after pumping a total of +/- 35 ml; which corresponds to 67% of the volume between tip of the paddle and disk. It is speculated that LCM channeled through the mud and plug the open slot. The P_{max} here reached 3000+ psi, which is the cell pressure limitation. This test had set a reference point for proceeding S_{circ} testing and assured the viability of the recipe.

For S_{circ} testing at 10 ml/min flowrate, Figure 5-3, the action of the stirring paddle had a dominant effect on both $V_{initial}$ and P_{max}; where were measured to be +/- 300 ml and +/- 500 psi respectively.
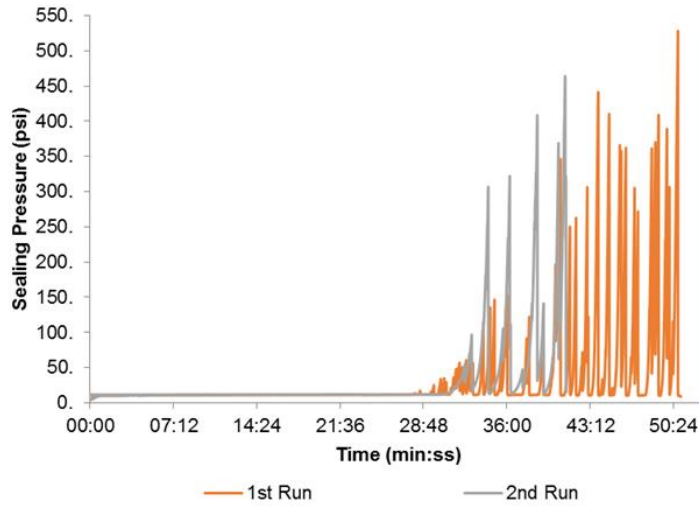
Figure V-3 S_{circ} Testing of 20 ppg NS & G TS1 @ 10 ml/min

Under the S_{circ} with 25 ml/min flowrate, $V_{initial}$ and P_{max} showed improvement over the lower

flowrate. P_{max} increased to +/- 1700 psi and $V_{initial}$ was measured to be 210 ml, Figure 5-4.
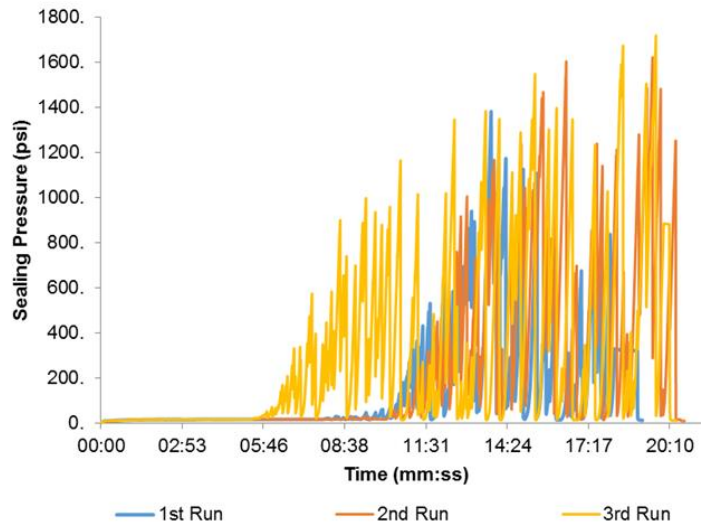

Figure V-4 S_{circ} Testing of 20 ppg NS & G TS1 @ 25 ml/min

With Further increase of flowrate, P_{max} and $V_{initial}$ continued to improve, Figure 5-5. P_{max}

recorded to be +/- 2980 psi with $V_{initial}$ at +/- 70 ml.
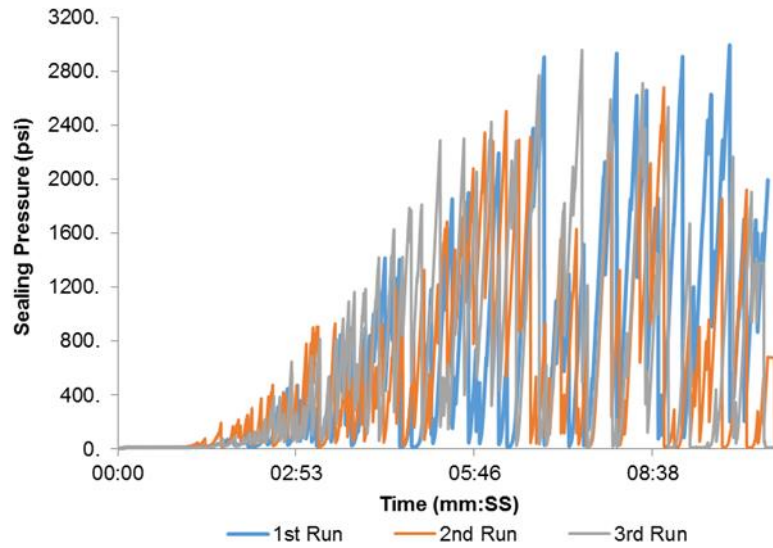
Figure V-5 D S$_{circ}$ Testing of 20 ppg NS & G TS1 @ 50 ml/min

Finally, as the flowrate increased to 75 ml/min the S$_{circ}$ effect was considerably undermined and the sealing behavior starts to follow the conventional one, Figure 5-6.
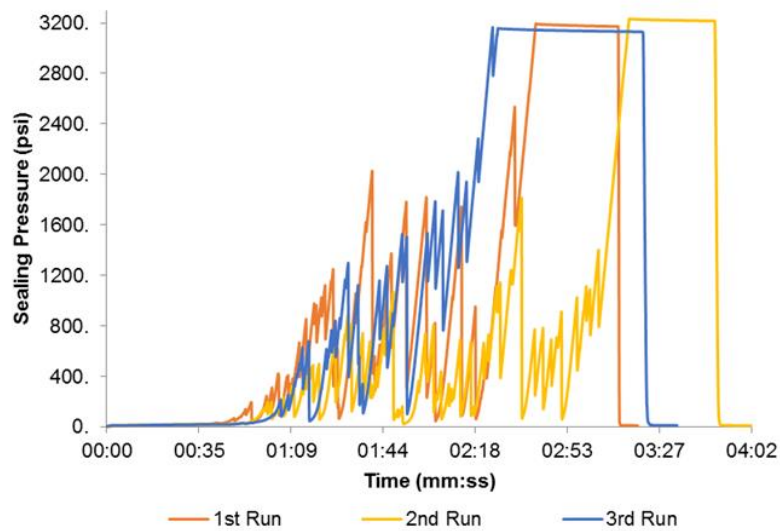

Figure V-6 S$_{circ}$ Testing of 20 ppg NS & G TS1 @ 75 ml/min

For a better visualization of data, Pressure Vs. Volume was plotted for the entire data set and presented below in Figure5-7.
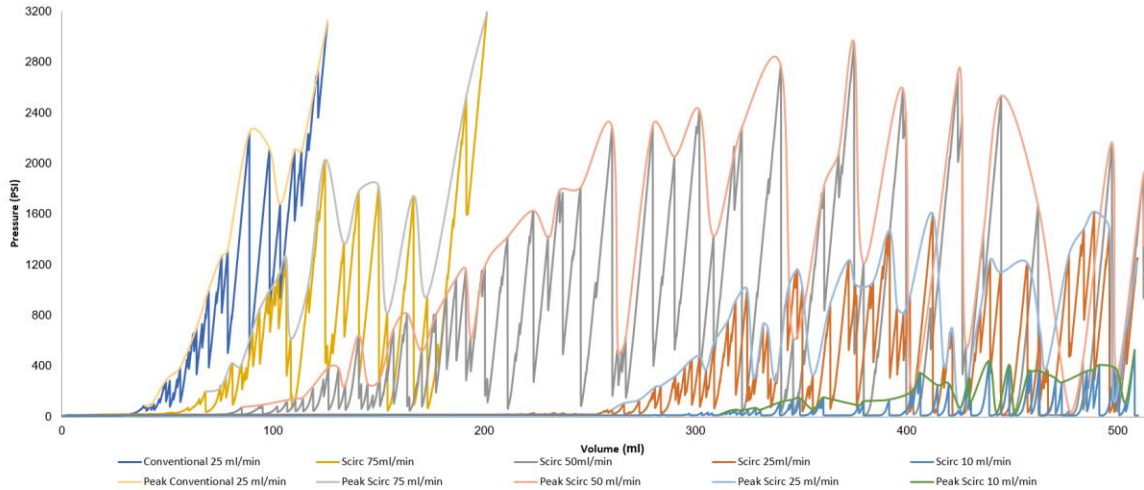
Figure V-7 TS1 G & NS Testing Set and Pressure Peak lines

The Figure demonstrates the effect of S_{circ} on the formation of the LCM seal. Under the S_{circ} with low flowrate, P_{max} recorded to be smaller in value and $V_{initial}$ are larger compared with conventional testing. As the flowrate increases the effect of S_{circ} is weakened and the seal starts to behave as conventional one.

When the recipe was tested on larger slot, TS4, S_{circ} effect was magnified. The sealing process was not initiated even at a flowrate of 25 ml/min; as opposed to a flowrate of 10 ml/min with TS1. The effect of S_{circ} here continued to play a major role where P_{max} experienced a considerable reduction in value, +/- 440 psi, even at flowrate as high as 125 ml/min when compared to conventional testing with P_{max} at +/-1300 psi. Figure 5-8 represents the data set in Pressure Vs. Volume plot.
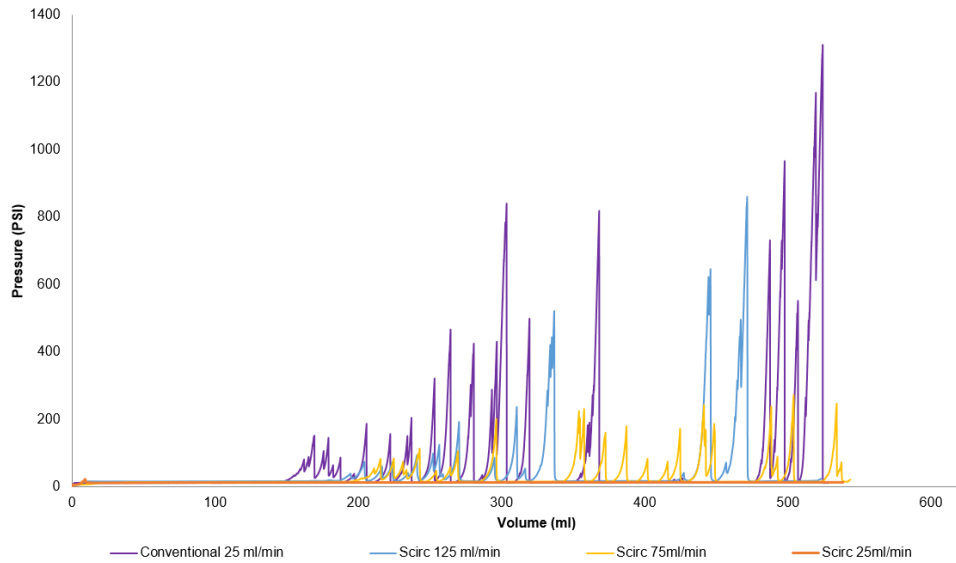
Figure V-8 40 ppg NS & G TS4 Test Set

GRAPHITE AND SIZED CALCIUM CARBONATES

G & SCC (1) LCM formulation was mixed in Mud 1 and tested on TS1 conventionally at a flowrate of 25 ml/min and under the S_{circ} at flowrates of 25, 75, 125 and 175 ml/min. Similar effect of thee S_{circ} was seen on both P_{max} and $V_{initial}$. However, the effect of the S_{circ} seemed to be more predominant; as the minimum flowrate to initiate a seal was rather high, 75 ml/min, and P_{max} seen a great reduction in value even at very high flowrate of 175 ml/min. Figure 5-9 represents the data set in Pressure Vs. Volume plot.

Figure V-9 105 ppg G & SCC TS1 Test Set

33

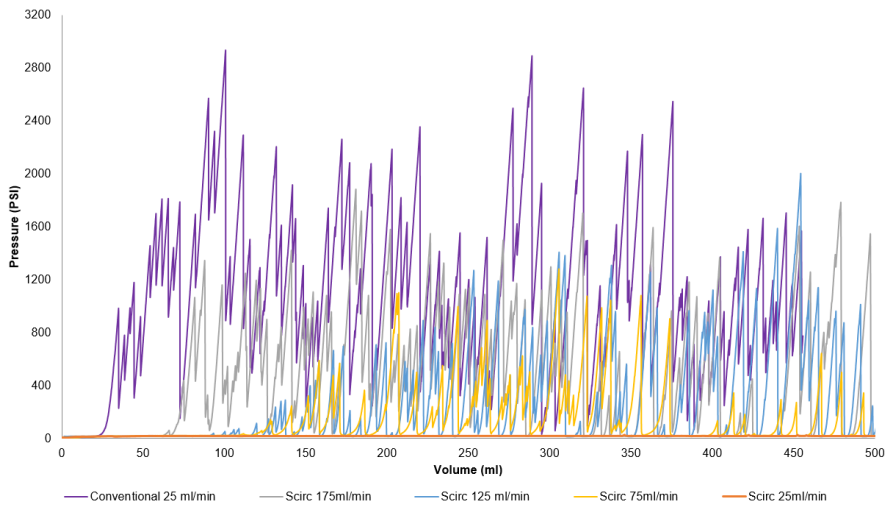When the LCM formulation of SCC & G (2) was tested on TS4 under the S_{circ}, a very high flowrate of 100 ml/min was required for a seal to initiate. The effect of the S_{circ} on fluid loss continued to be observed as higher flowrate corresponded to lower $V_{initial}$. However, P_{max} did not seem to be effected, Figure 5.10 illustrates the Pressure Vs. Volume plot.
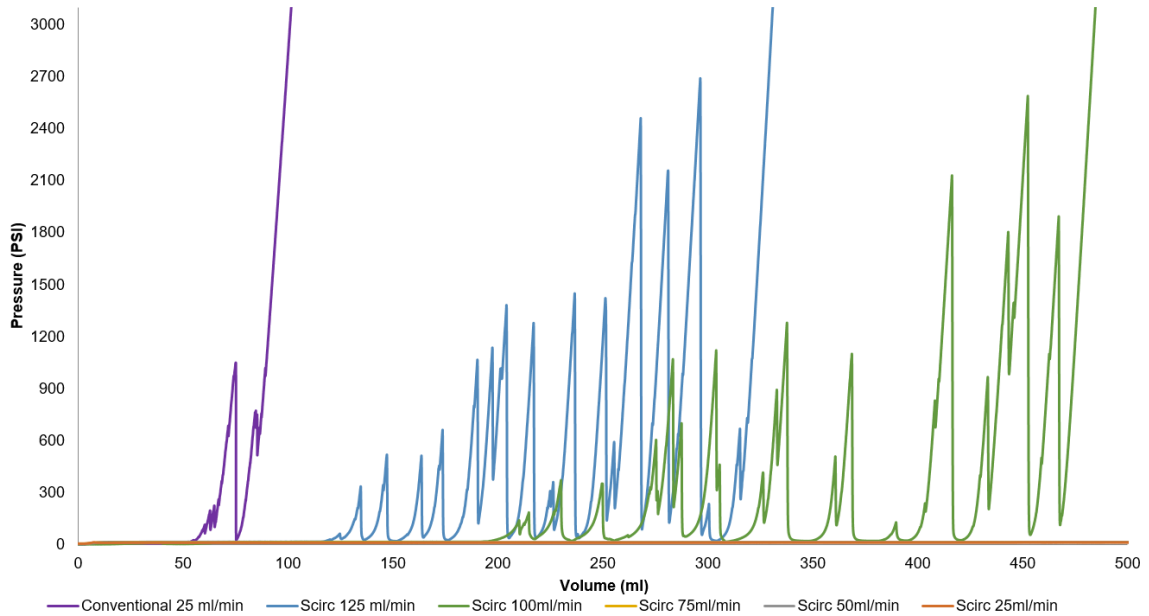
Figure V-10 105 ppg G & SCC TS4 Test Set

To explain such an observation, the seals of Conventional and S_{circ} testing were investigated (Figure 5-11). In conventional testing the LCM particles found to be screened out at the fracture surface, Figure 5-11 I, while with the S_{circ} testing the LCM particles wedged inside the slot, Figure 5-11 II, and formed more of a realistic seal. Another explanation can be tied to the way the seals are evaluated, only recording P_{max}, which can mask any variation in seal integrity.

Figure V-11 I. Conventional Testing Seal II. S$_{circ}$ Seal

GRAPHITE, SIZED CALCIUM CARBONATES AND CELLULOSIC FIBER

The recipe was tested conventionally at a flowrate of 25 ml/min and under the S$_{circ}$ at flowrates of 25, 50 and 75 ml/min. The conventional testing continued to record highest P_{max} and lowest $V_{initial}$. Similar to NS & G LCM formulation, the S$_{circ}$ effect was dominant at low flowrate and lessened as flowrate increases. The results of the testing are presented below in Figure 5-12.
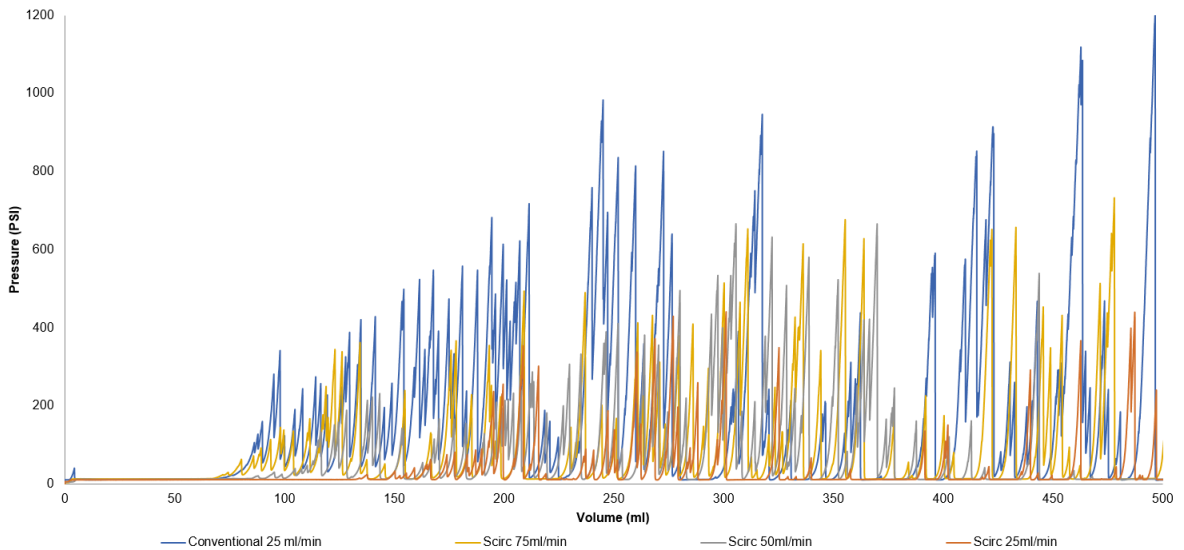

Figure V-12 55 ppg G & SCC & CF TS1 Test Set

ANALYSIS FOR FIELD IMPLICATIONS

Traditionally, the maximum pressure observed during LCM experiments is reported as the main outcome (Al-saba et al., 2014 a,b ; Kumar et al., 2011). In this study 100 psi and higher pressure peaks, resembling competent seal, leading to the maximum pressure were considered in order to address the behavior of the developed LCM plug. Figure 5-7 illustrates this concept for TS1 G & NS testing set. To model the relationship between the sealing pressure in (PSI) and fluid loss volume in (ml), a linear regression approach intercepting the origin was used, (Figure 5-13).
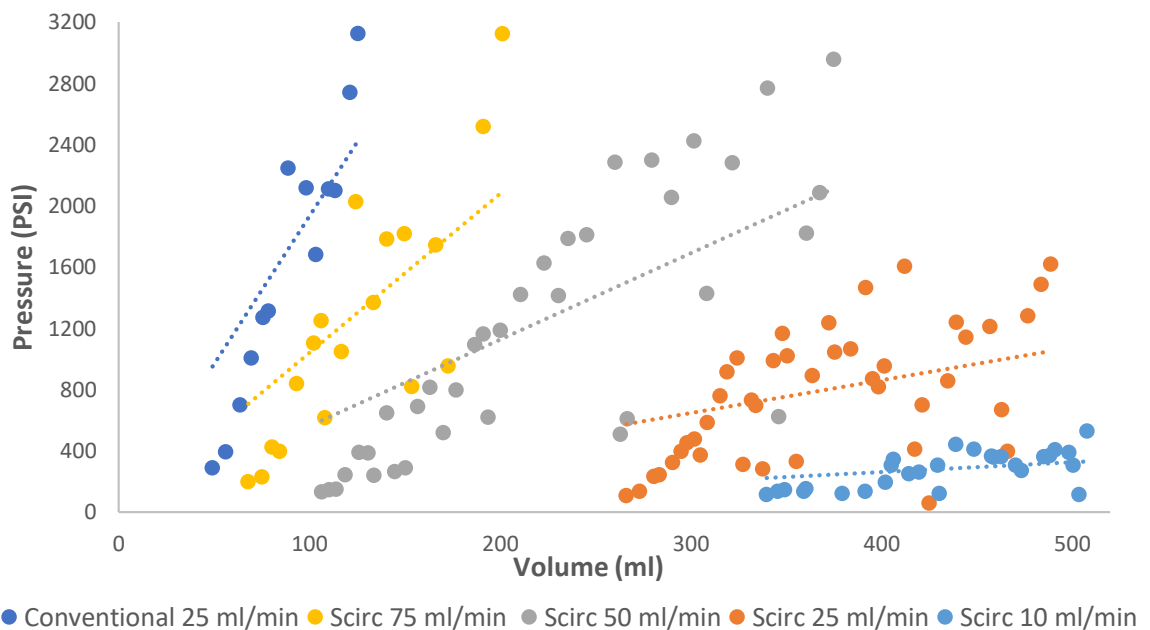
Figure V-13 TS1 NS & G Testing Set Linear Regression

By normalizing the linear regression slopes with respect to conventional testing, a relationship between S_{circ} and conventional condition was established. The established relationship defines the sealing effectiveness ratio (SER) which is believed to better represents the sealing integrity of the LCM plug under a S_{circ}. The SER can be used to resemble the S_{circ} effect by degrading the conventional testing maximum sealing pressure of a given LCM recipe. Figure 5-14 sums up all the SER's of the tested LCM recipes under various flowrates.

Figure V-14 Sealing Effectiveness Ratio

Figure 5-14 shows that under the S_{circ} the LCM recipes responded differently to the changing of flowrates. For example, at a flowrate of 100 ml/min the TS4 SCC & G LCM formulation lost about 80%, SER of 0.22, of its conventional testing maximum sealing pressure. In addition, the figure shows that the LCM formulation that contains NS, lo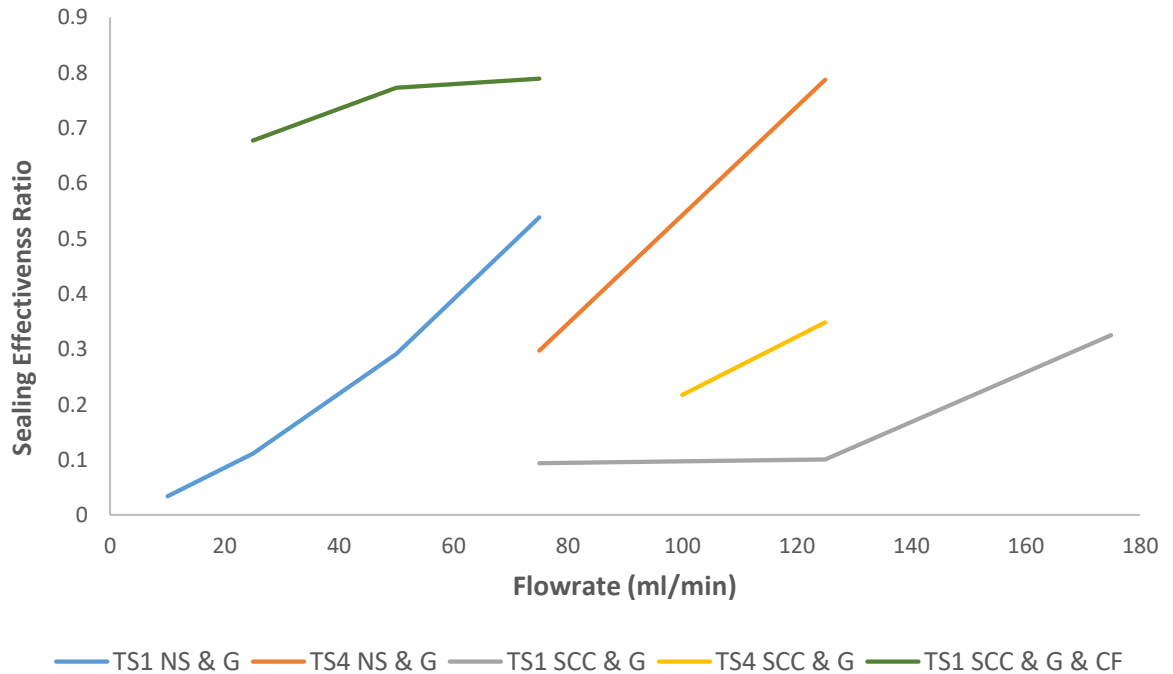w specific gravity, required low flowrate for a seal to initiate and yields a high SER's under S_{circ}; as opposed to SCC formulations with relatively high specific gravity

To tie up these observations and findings to field implication, fluid flow in a wellbore is considered. When losses occur in a wellbore, the drilling mud flows into two directions 1) up the wellbore annulus, 2) into the fracture or thief zone. These two competing perpendicular crossflows are simulated in the developed apparatus through the stirring action of the paddle and the mud movement via syringe pump respectively. The changing in flowrates mimics the severity of LC and undermines the effect of stirring action or fluid movement up the annuals. Thus, the study can be used to evaluate the effectiveness of LCM formulation as sweep or preventive treatments. All the tested LCM formulations lost a percentage of their maximum sealing pressure

under the S_{circ}. Therefore, the practice of sweeping the hole with LCM pill at drilling flowrate is not recommended. In addition, it can be concluded that NS LCM formulations are less prone to the S_{circ} making them better sweep and preventive treatment candidates.

VUGGY DISKS EXPERIMENT RESULTS

During the LPA screening stage, three different blends of LCMs have successfully initiated seals for the different EVD size disks. These blends were considered as potential effective LCM recipes and thus tested at higher differential pressure using the DFL&SET. Table 8 shows the formulations of these LCM blends.

EVD			5 mm		7.5 mm		10 mm		12.5 mm		5 -7.5mm			10-12.5 mm			All				
LCM Type			SCC	G & SCC Blend	SCC	G & SCC Blend	SCC	G & SCC Blend	SCC	G & SCC Blend	NS	SR	G	NS	SR	G	NS	G	FM	SF	ASF
LCM Concentration (ppb)			105								140			154			83				
LCM Size in Microns	D(50) microns	50											4.9%			4.5%	8.2%				
		100											4.9%			4.5%	8.2%				
		400											7.3%			6.7%	12.5%				
		500		20.0%		20.0%		20.0%		20.0%											
		620									8.1%			7.3%			13.7%				
		750	5.0%		5.0%		5.0%														
		1000											7.3%			6.7%	12.5%				
		1200	12.5%		5.0%				5.0%												
		1400	12.5%		10.0%		12.5%														
		1450									8.1%			7.3%			13.7%				
		1850	12.5%						12.5%			3.9%			5.4%						
		2077																			11.1%
	% of total concentration	2180										3.9%			3.6%						
		2300									8.3%			7.6%			14.0%				
		2500	12.5%		10.0%		12.5%		12.5%												
		3180	7.5%		12.5%		7.5%					3.9%			5.4%						
		4380	7.5%		12.5%		7.5%					4.7%			5.4%						
		5180	10.0%		7.5%		10.0%		12.5%			4.7%			3.6%						
		5950			7.5%							4.7%			3.6%						
		6500					7.5%		12.5%			5.5%			5.4%						
		7350			10.0%		7.5%					6.3%			5.4%						
		8750					10.0%		15.0%			6.3%			5.7%						
		10350							10.0%			7.1%			5.7%						
		11850														6.4%					
	Exact Size	3000																0.6%		
		10000																1.2%		
		12500																	3.2%	
		25400																1.2%		

Table 8 Potential LCM Recipes

A total of 21 tests were conducted on these potential blends at higher pressure, as per test procedure and methodology presented earlier, to identify effective LCM treatments and verify

testing conditions. The results are summarized in Table 9 which lists the following for each test: LCM blend, opening size thickness and shape of used disk, testing condition, drilling fluid type and density in lb/gal, total LCM concentration in ppb, and the maximum sealing pressure in psi. Six tests were repeated to evaluate repeatability and they showed sealing pressure accuracy of +/- 15%; which is in alignment with a detailed study of accuracy of slot disk by Jeennakorn et al., (2017).

Test #	LCM Blend	Size (mm)	Thickness	Opening Type	Test Condition	Drilling Fluid	Density (lb/gal)	Concen. PPB	Maximum Sealing Pressure PSI
1	SCC & G	5				Mud 2	15.4	105	3000+
2		7.5							3000+
3		10							3000+
4		12.5							3000+
5									2500
6	NS & SR &G	5	.25 in	Irregular Shape	Constant Pressure	Mud 1	8.7	140	797
7									1,013
8		7.5							415
9									473
10		10						154	368
11		12.5							234
12	NS & G & FM & SF & ASF	5						83	1,383
13		7.5							1,433
14		10							1,229
15		12.5							1,049
16	NS & SR &G	5		Strait Slot				140	447
17									452
18		7.5							540
19			1 in	Irregular Shape					587
20		7.5			Constant Flow rate				273
21									379

Table 9 High Pressure Test Results

Out of the three blends, SCC & G recipe gave the highest sealing pressure for all EVD sizes at pressure exceeding 3,000 psi; which is the cell pressure limitation. The results of the 12.5 mm EVD disk is plotted below as Pressure Vs. Time in Figure 5-15:
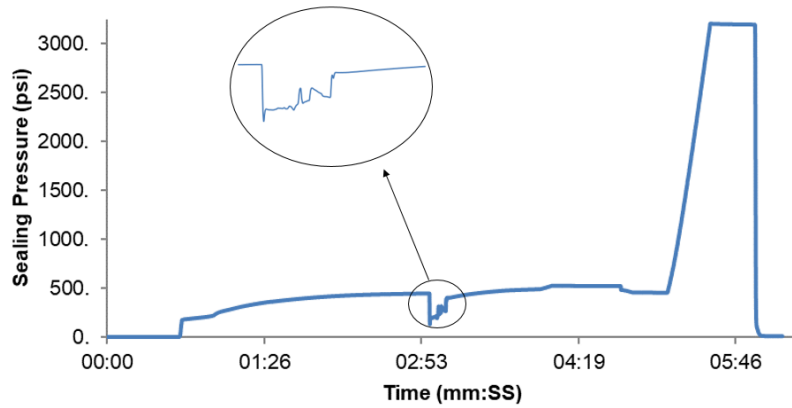
Figure V-15 105 ppb SCC & G LCM Blend, 12.5 mm EVD Disk

As illustrated, the cell was first pre-pressured to +/- 300 psi prior to allowing fluid to flow

through the vuggy disk at +/- 2:53 min. Once the test commenced, the process of seal initiation

started to take place, magnified in the graph, until impermeable seal is formed. The test is then

continued in constant flow mode and seal was brought to maximum differential pressure of 3000

psi. Similar results were found for all other disks.

In NS & SR & G LCM blend, the maximum sealing pressure varies depending on the EVD; as

the EVD increased the maximum sealing pressure decreased. Figure 5-16 below shows the

Pressure Vs. Time graph for 5 mm EVD disk.

Figure V-16 140 ppb NS & SR & G LCM Blend, 5 mm EVD Disk

40

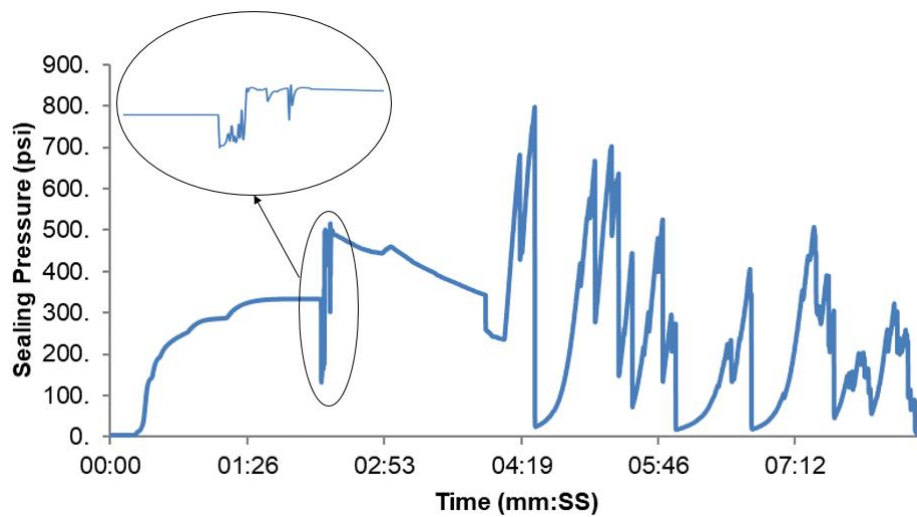For this LCM blend more peaks were observed prior to the formation of the impermeable seal (Figure 5-16) when compared to previous blend (for instance Figure 5-15). To explain such a behavior, the two different seals were examined and compared. It can be observed in Figure 5-17 that the two seals were formed differently. In Figure 5-17 a & b, the LCM wedged inside the irregular shape openings and formed a plug while in Figure 5-17 c & d the LCM screened out at the surface of the disk. Such a difference in seal formation would have an effect in the sealing process. It appears that the multiple peaks are formed due to a more complicated sealing process.
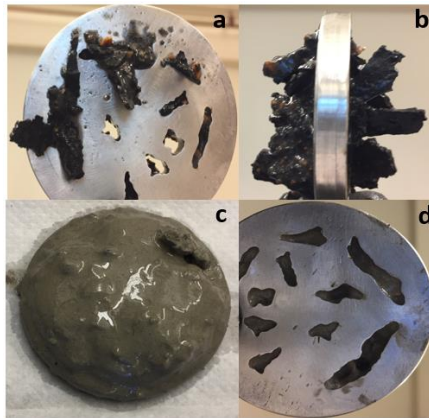
Figure V-17 a & b. NS & SR & G Seal. c& d. SCC & G Seal

It worth mentioning here that the durometer hardness reading for the synthetic rubber (SR) used was approximately 60A and the effect of temperature was not investigated as it was outside the scope of this work.

The high pressure evaluation of LCM blend # 3 was similar to recipe # 2; where seal initiation process had multiple peaks and the formed seal wedged inside the vugs. However, the maximum sealing pressure for this LCM recipe was much higher for the larger EVD disks. As an example, the 10 mm EVD disk, presented in Figure 5-18, had maximum sealing pressure of 1229 psi which makes it a better potential treatment.

Figure V-18 83 ppb NS & G & FM & SF & ASF LCM blend, 10 mm EVD

TESTING CONDITIONS OF THE VUGGY EXPERIMENT

To validate the testing methodology and procedure used in this set of experiments, testing conditions were altered, high pressure testing was conducted and maximum sealing pressures were observed for any variation. The subsections below helped in the determination of the ideal testing conditions that best simulates remedial treatment in vugular formations.
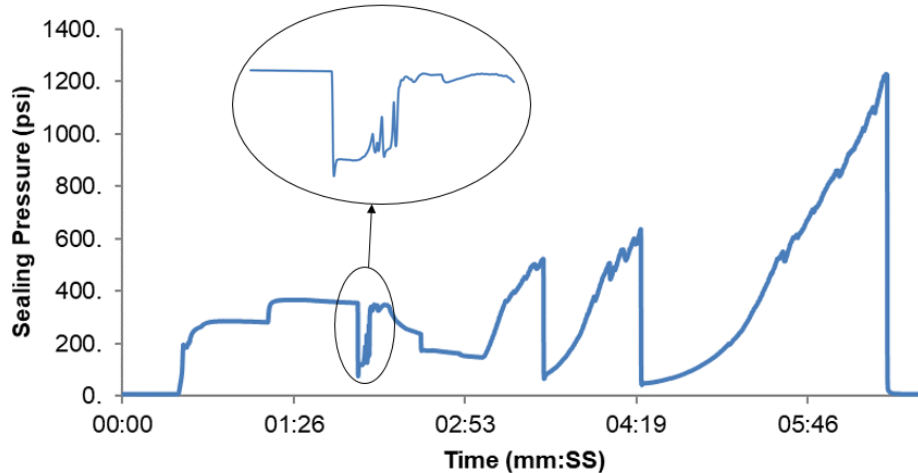
VUGGY VS. STRAIT SLOT DISKS

To justify the use of irregular shape opening disks and identify if a different sealing pressure and process exists, high pressure tests were conducted on 5 mm strait slot (SS) disk; used to simulate fractures. The results were then compared to the 5 mm EVD disk. Tests# 6,7, 16 and 17 in Table 9 clearly indicate that using 5 mm EVD disk would result in higher sealing pressure. When the formed seals were investigated, SR found to be wedged a lot easier in irregular shape openings, shown in Figure 5-19, resulting in the higher pressure observed.
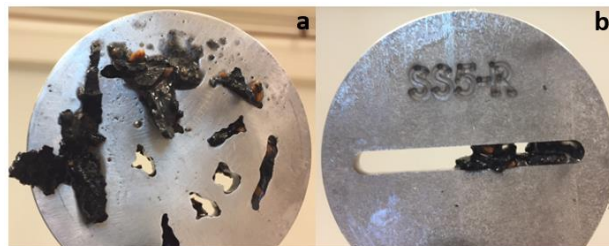

Figure V-19 a. 5 mm Vuggy disk b. 5mm Strait slot disk

1 in VS. 0.25 in DISKS

To investigate if thickness would have an effect on the sealing pressure, a 7.5 mm EVD disk was manufacture with 1" in thickness, as opposed to 0.25" for the base design. Figure 5-20 shows the two disks.

Figure V-20 1 inch and 0.25 inch Thick 7.5 mm EVD disks

The 1-inch disk was tested at high pressure using recipe # 2 and the results were compared to the base design. Tests# 8, 9, 18 and 19, shown in Table 9, indicate when the 1-inch disk was used, 15-40% improvement in sealing pressure was achieved. This means using 0.25 inch disks resulted in an under estimation of the actual sealing capability of the tested recipes. Also, it can be concluded that vugular formation are better simulated through the use of 1 in disks.

CONSTANT PRESSURE VS. CONSTANT FLOWRATE

All performed high pressure LCM laboratory testing was conducted at constant pressure mode; to simulate overbalance condition. The validity of this approach was examined here through testing recipe # 2 in constant flowrate mode. The cell was not pre-pressure this time and seals were left to initiate with a flowrate of 25 ml/min. The results of both modes, shown in Tests# 18, 19, 20 and 21of Table 9, were then compared. The results illustrate higher sealing pressures when recipes were tested under constant pressure mode. Since drilling overbalance is the common drilling practice, constant pressure mode will better simulate the actual field condition. Thus testing with constant pressure mode is encouraged to be used in all vugular LCM testing.

CHAPTER VI

CONCLUSION

- Simulated fluid circulation along the wellbore has a dominant effect on the sealing integrity of LCM recipes. When comparing to conventional testing, higher fluid loss volumes and lower sealing pressures were recorded.

- The effect of S_{circ} seen in the experiments is lessened when flowrate increases and overcomes the crossflow force.

- The increase of slot size amplified the effect of the S_{circ}. For a given recipe, higher fluid loss volumes with lower sealing pressures were seen for the larger disk TS4.

- Using the developed apparatus, the Dynamic Fluid Loss & Seal Efficiency Tester, yields a potentially more reliable result as LCM particles are prevented from screening at the fracture surface; forming a false seal.

- The study indicates that LCM treatments lose a high percentage of their maximum sealing pressure under a S_{circ}. Hence, the practice of sweeping the hole with LCM pill at high flowrate while drilling may not actually cause the LCM to move into the fractures. The laboratory results indicate that spotting LCM pills at the bottom of the hole at low flowrates yields a higher chance in curing the losses.

- The used LCM recipes responded differently to the S_{circ}. Recipes with lower specific gravity materials found to be less susceptible to the S_{circ}; making them better preventive approach candidates.

- The study highlights the importance of PSD for the sealing process and encourages the industry to invest more in developing of large enough LCM sizes to cure losses in vugular formation.

- Three blends of LCM found to be effective in sealing the vuggy disks, simulating vuggy formation, with a maximum sealing pressure reaching as high as + 3000 psi.

- Depending on the LCM properties, the seal can either forms and wedges inside the irregular shape openings or screens and forms as a thick chunk at the surface of the disk.

- The use of vuggy disks yields a higher maximum sealing pressure and believed to better simulate vugular formation.

- A higher maximum sealing pressure was recorded when LCM recipes were tested in 1 in thick disk under a constant pressure mode, which is believed to better represent the actual field performance of these LCM recipes.

CHAPTER VII

FUTURE WORK RECOMMENDATION

- The effect of S_{circ} on LCM seal integrity, shown in the experiment, highlighted the major role played by fluid flow in a wellbore (i.e. fluid flow up the hole, and fluid flow into the loss zone). However, a relationship between the laboratory condition, fluid movement caused by syringe pump flowrate and stirring action, and field condition, the two fluid flow patterns, has not been established. It is the author recommendation to pursue such a relationship so that the field performance of LCM recipes can be better predicted.

- The simulation of vuggy formation using irregular shape opening disks is a quite new concept with a lot of potential emphasis. For example, the effect of higher overbalance condition was not considered. Also the effect of the variation in vuggy disks flow areas on the seal integrity was not considered. An investigation of such inconsistency is highly recommended.

REFERENCES

Aadnoy, B. S., Belayneh, M., Arriado Jorquera, M. A., & Flateboe, R. (2008, September 1). Design of Well Barriers To Combat Circulation Losses. Society of Petroleum Engineers

Aadnoy, B. S., Mostafavi, V., & Hareland, G. (2009, January 1). Fracture Mechanics Interpretation of Leak-Off Tests. Society of Petroleum Engineers.

Abrams, A., "Mud Design to Minimize Rock Impairment due to Particle Invasion", J. Pet. Tech, May, 1977, 586-592.

Alberty, M. and McLean, M. (2004). A Physical Model for Stress Cages. SPE Annual Technical Conference and Exhibition.

Al Menhali, S., Abdul Halim, A. O., & Al Menhali, S. (2014, November 10). Curing Losses While Drilling & Cementing. Society of Petroleum Engineers. doi:10.2118/171910-MS

Alsaba, M., Aldushaishi, M., Nygaard, R., and Nes,O. (2016). Updated criterion to select particle size distribution of lost circulation materials for an effective fracture sealing. Journal Of Petroleum Science and Engineering.

Al-saba, M., Nygaard, R., Saasen, A. and Nes, O. (2014). Lost Circulation Materials Capability of Sealing Wide Fractures. SPE Deepwater Drilling and Completions Conference.

Al-saba, M., Nygaard, R., Saasen, A. and Nes, O. (2014). Laboratory Evaluation of Sealing Wide Fractures Using Conventional Lost Circulation Materials. SPE Annual Technical Conference and Exhibition.

Alshubbar, G., D., Nyggard, R. (2018). Curing Losses in Vuggy Carbonate Formations. SPE/IADC Middle East Drilling Technology Conference and Exhibition.

Aston, M. S., Alberty, M. W., McLean, M. R., de Jong, H. J., & Armagost, K. (2004, January 1). Drilling Fluids for Wellbore Strengthening. Society of Petroleum Engineers.

Baldino, S., Osgouei, R., Ozbayoglu, E., Miska, S., Takach, N., May, R. and Clapper, D. (2015). Cuttings Settling and Slip Velocity Evaluation in Synthetic Drilling Fluids. 12Th Offshore Mediterranean Conference and Exhibition.

Bybee, K. (2008, January 1). Wellbore-Strengthening Technique for Drilling Operations. Society of Petroleum Engineers. doi:10.2118/0108-0067-JPT

Contreras, O., Hareland, G., Husein, M., Nygaard, R., & Alsaba, M. (2014, September 10). Wellbore Strengthening In Sandstones by Means of Nanoparticle-Based Drilling Fluids. Society of Petroleum Engineers

Dick, M. A., Heinz, T. J., Svoboda, C. F., & Aston, M. (2000, January 1). Optimizing the Selection of Bridging Particles for Reservoir Drilling Fluids. Society of Petroleum Engineers.

Dupriest, F. (2005). Fracture Closure Stress (FCS) and Lost Returns Practices. SPE/IADC Drilling Conference.

Dupriest, F. E., Smith, M. V., Zeilinger, S. C., & Shoykhet, N. (2008, January 1). Method To Eliminate Lost Returns and Build Integrity Continuously With High-Filtration-Rate Fluid. Society of Petroleum Engineers. doi:10.2118/112656-MS

Fang, G. (1992). An Experimental Study of Free Settling of Cuttings in Newtonian and Non-Newtonian Drillings Fluids: Drag Coefficient and Settling Velocity. Society of Petroleum Engineers Journal.

Hettema, M., Horsrud, P., Taugbol, K., Friedheim, J., Huynh, H., Sanders, M. and Young, S. (2007). Development of an Innovative High-Pressure Testing Device for the Evaluation of Drilling Fluid Systems and Drilling Fluid Additives within Fractured Permeable Zones. Offshore Mediterranean Conference and Exhibition.

Hidajat, I., Mohanty, K., Flaum, M., & Hirasaki, G. (2004). Study of Vuggy Carbonates Using NMR and X-Ray CT Scanning. SPE Reservoir Evaluation & Engineering, 7(05), 365-377.

Kumar, A., Savari, S., Whitfill, D., & Jamison, D. E. (2010, January 1). Wellbore Strengthening: The Less-Studied Properties of Lost-Circulation Materials. Society of Petroleum Engineers.

Fuh, G.-F., Morita, N., Boyd, P. A., & McGoffin, S. J. (1992, January 1). A New Approach to Preventing Lost Circulation While Drilling. Society of Petroleum Engineers. doi:10.2118/24599-MS

Ghalambor, A., Salehi, S., Shahri, M. and Karimi, M. (2014). Integrated Workflow for Lost Circulation Prediction. SPE International Symposium and Exhibition on Formation Damage Control.

Kumar, A., Savari, S., Jamison, D. and Whifill, D. (2011). Application of Fiber Laden Pill for Controlling Lost Circulation in Natural Fractures. AADE National Technical Conference and Exhibition.

Kumar, A., Savari, S. (2011, April) Lost Circulation Control and Wellbore Strengthening: Looking Beyond Particle Size Distribution. AADE National Technical Conference and Exhibition, Houston.

Lucia, F. (2007). Carbonate reservoir characterization. Berlin: Springer.

Morita, N., Black, A. D., & Guh, G.-F. (1990, January 1). Theory of Lost Circulation Pressure. Society of Petroleum Engineers. doi:10.2118/20409-MS

Murphy, R., Jamison, D., Hemphill, T., Bell, S. and Albrecht, C. (2006). Apparatus for Measuring the Dynamic Solids Settling Rates in Drilling Fluids. SPE Annual Technical Conference and Exhibition.

M7150 Stirred Fluid Loss Tester | Grace Instrument®. (2017). Graceinstrument.com. Retrieved 22 October 2017, from http://www.graceinstrument.com/M7150.php

Onyia, E. C. (1991, January 1). An Analysis of Experimental Data on Lost Circulation Problems While Drilling With Oil-Base Mud. Society of Petroleum Engineers. doi:10.2118/22581-MS

Powell, J., Parks, C. and Seheult, J. (1991). Xanthan and Welan: The Effects of Critical Polymer Concentration On Rheology and Fluid Performance. International Arctic Technology Conference

Salehi, S., & Nygaard, R. (2010, January 1). Finite-element Analysis of Deliberately Increasing the Wellbore Fracture Gradient. American Rock Mechanics Association.

Salehi, S., & Nygaard, R. (2011, January 1). Numerical Study of Fracture Initiation, Propagation, Sealing to Enhance Wellbore Fracture Gradient. American Rock Mechanics Association

Salehi, S., & Nygaard, R. (2011, January 1). Evaluation of New Drilling Approach for Widening Operational Window: Implications for Wellbore Strengthening. Society of Petroleum Engineers. doi:10.2118/140753-MS

Salehi, S., & Nygaard, R. (2012, January 1). Numerical Modeling of Induced Fracture Propagation: A Novel Approach for Lost Circulation Materials (LCM) Design in Borehole Strengthening Applications of Deep Offshore Drilling. Society of Petroleum Engineers. doi:10.2118/135155-MS

Sanders, M., Young, S. and Friedheim, J. (2008). Development and Testing of Novel Additives for Improved Wellbore Stability and Reduced Losses. AADE Fluids Conference and Exhibition.

Savari, S., Whitfill, D., Jamison, D. and Kumar, A. (2014). A Method to Evaluate Lost Circulation Materials - Investigation of Effective Wellbore Strengthening Applications. IADC/SPE Drilling Conference and Exhibition.

Van Oort, E. and Vargo, R. (2008). Improving Formation-Strength Tests and Their Interpretation. SPE Drilling & Completion, 23(03), pp.284-294.

Van Oort, E., Friedheim, J., Pierce, T. and Lee, J. (2009). Avoiding Losses in Depleted and Weak Zones by Constantly Strengthening Wellbores. SPE Annual Technical Conference and Exhibition.

Wang, H., Towler, B., Soliman,M. (2007). Fractured Wellbore Stress Analysis: Sealing Cracks to Strengthen a Wellbore. Society of Petroleum Engineers.

Wang, H., Soliman, M. Y., & Towler, B. F. (2008, January 1). Investigation of Factors for Strengthening a Wellbore by Propping Fractures. Society of Petroleum Engineers.

Wang, H. M., Savari, S., Whitfill, D. L., & Yao, Z. (2016, March 1). Forming a Seal Independent of Formation Permeability to Prevent Mud Losses - Theory, Lab Tests, and Case Histories. Society of Petroleum Engineers.

Xu, C., Kang, Y., You, L., Li, S., & Chen, F. (2014, September 1). High-Strength, High-Stability Pill System To Prevent Lost Circulation. Society of Petroleum Engineers.

Zakaria, A., Sayed, M., & Nasr-El-Din, H. (2012). Propagation of Emulsified Acids in Vuggy Dolomitic Rocks. SPE Kuwait International Petroleum Conference And Exhibition.

APPENDICES

A. WELLBORE STRENGTHENING MECHANISM

Wellbore strengthening (WS), or curing losses in fractured formations, might be a conceiving term as it presumes some strength gain to the rock matrix. As a matter of fact, the strength remains unchanged. However, other influences are behind the ability of the wellbore to withstand higher pressures. Some researchers refer to the concept as "Drilling margin extension" (Van Oort et al., 2009). Fuh simply defines WS as "when the breakdown pressure of the wellbore is greater after the treatment than before the losses initiated" (Kybee, 2008). Others define the term as "a set of techniques used to efficiently plug and seal induced fractures while drilling to deliberately enhance the fracture gradient and widen the operational window" (Salehi and Nygaard, 2012). Regardless of the definition, a higher mud weight can be used after the treatments resulting in less casing strings, widening narrow mud window, and ultimately prevent loss circulation.

The history of WS goes back to the 1980's with the DEA-13 project; where difference in formation breaking pressure (P_{bd}) between water based mud (WBM) and oil/synthetic based mud (O/SBM) was found which was tied to the difference in mud filter cake. Onyia (1991) has also conducted a study focuses particularly on this phenomenon. A decade Later, a joint industry project between GPRI and M-I SWACO was carried out in hope to revive DEA-13. However, in smaller scale to screen out effective wellbore Strengthening materials (WSM). One of the most important finding was the identification of synthetic graphite as an effective WSM. These two projects have set the bases of the two main schools of thoughts:

- Wellbore-Stress Augmentation (WSA).
- Fracture Propagating Resistance.

Each one of these mechanisms will be explained individually along with some recently added WS Mechanisms.

Stress Caging.

This is the first suggested WSA mechanism in which additional hoop stress thought to be created. The principle of stress caging is "to deposit solids at or close to the mouth of a newly formed fracture which will act both as a proppant and as a seal isolating the fluid pressure in the wellbore from the majority of the fracture. Provided the formation is sufficiently permeable, pressure beyond the blockage will dissipate ultimately to the formation pore pressure. Thus, the fracture will attempt to close which increases the hoop stress in excess of its original value", (Alberty and McLean, 2004). Figure 1illustrate this concept.
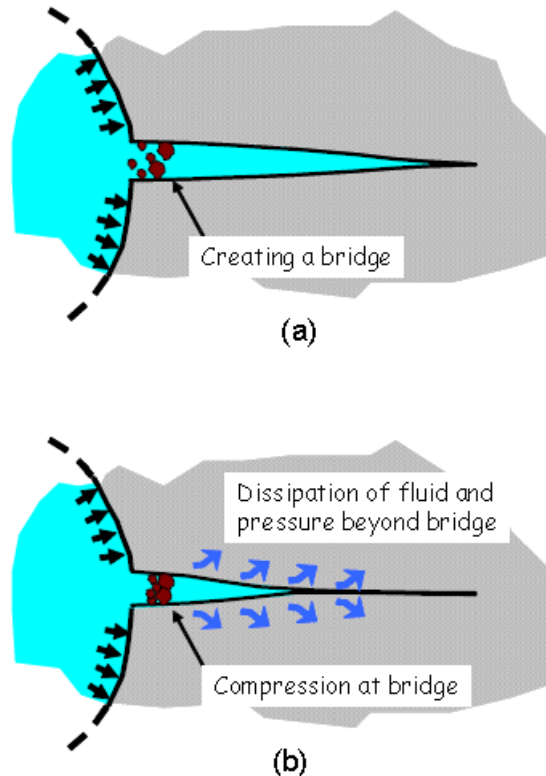

Figure A1: Stress Cage process (Alberty and McLean, 2004).

To highlight the important parameters that paly a rule in WSA, Aston et al. (2004) assumes a radial fracture and used an equation from fracture stimulation theory to find the pressure needed to keep a fracture open with certain width:

$$\Delta P = \frac{\pi}{8} * \frac{w}{R} * \frac{E}{(1-v^2)} \quad (1)$$

Even though this equation is not feasible to be used to calculate the expected WS, due to the physical difference of how pressure and the blockage works, it shows the same relationship between Young's modulus and fracture width. The idea of arresting the fracture as soon as possible is probably obtained from above equation as well; radial distance, R, is inversely related to change in pressure. Lab experiments were done to investigate the following variables:

- Rock permeability
- Mud Type & weight

- Temperature
- Mud injection pressure
- Bridging type, concentration, PSD
- Fracture width

To identify parameters that have a major effect on both fracture width and WS, Alberty and Mclean (2004) used a numerical model approach. Their study identified the following parameters:

- Location of the blockage
- Pore pressure
- Stress anisotropy
- Young's modulus

PSD and concentration were determined by calculating the fracture volume through assuming a triangular prism shaped fracture:

$$V_F = \frac{1}{2}Lw^2 \ (2)$$

A 2D plane strain and linear elastic boundary element analysis (BEA) approach was used by Wang et al., (2007; 2008) to investigate the factors, listed below, that effects the hoop stress while maintaining a stable fracture:

- Fracture Pressure
- Fracture Width (Crack Opening Displacement (COD)
- Fracture Length
- Wellbore Radius
- Elastic Properties
- Propping location

The numerical study showed that hoop stress can be increase beyond Kirsch equation, an analytical estimation of fracturing pressure, Figure 2.
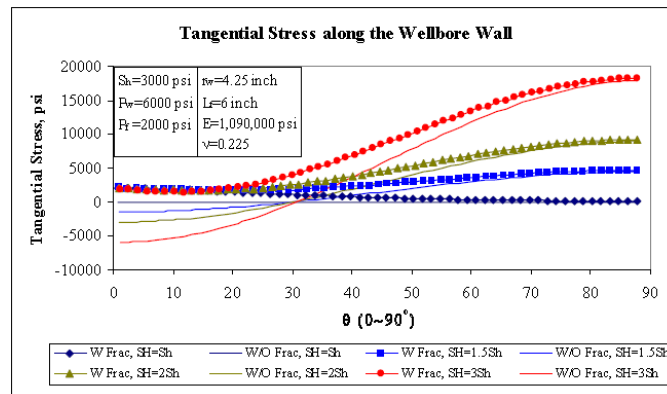

Figure A2: Hoop stress at wellbore wall Wang et al., (2007)

In the contrary to Astons conclusions with respect to fracture length investigation, a miner effect on the amount of hoop stress was observed at small stress anisotropy, Figure 3.
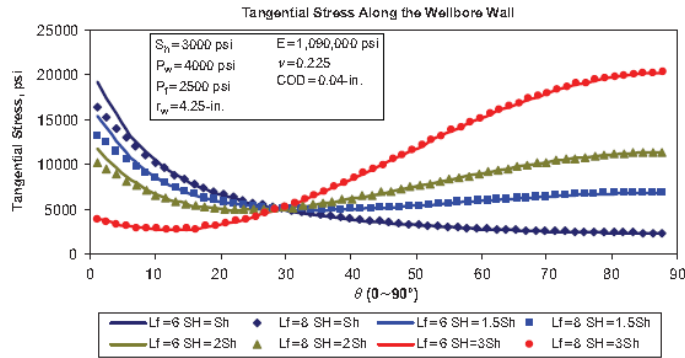

Figure A3: Hoop stress Vs. Fracture length Wang et al., (2007)

Alberty and Mclean (2004) also observed that the fracture is more stable, as shown it Table 2.

S_H (psi)	S_h (psi)	P_w (psi)	P_f (psi)	E (psi)	v	L_f (in.)	COD (in.)	K_I (psi-in.$^{0.5}$)
3000	3000	4000	2500	1090000	0.225	6	0.04	1019
3000	3000	4000	2500	1090000	0.225	8	0.04	492
4500	3000	4000	2500	1090000	0.225	6	0.04	1030
4500	3000	4000	2500	1090000	0.225	8	0.04	403
6000	3000	4000	2500	1090000	0.225	6	0.04	1041
6000	3000	4000	2500	1090000	0.225	8	0.04	313
9000	3000	4000	2500	1090000	0.225	6	0.04	1063
9000	3000	4000	2500	1090000	0.225	8	0.04	134

TABLE 4—STRESS INTENSITY FACTORS AFFECTED BY FRACTURE LENGTH AND STRESS ANISOTROPY

Table A1: Effects of Fracture Length on KI Alberty and Mclean (2004)

For more information on the other effects please refer to the Alberty and Mclean (2004) SPE papers

Despite the popularity of Stress Caging theory, some researchers challenge this principle. The study by Salehi and Nygaard (2011) showed that the wellbore strengthening approach only restores the wellbore hoop stress back to its ideal case defined by kirsch equation, Figure 4.
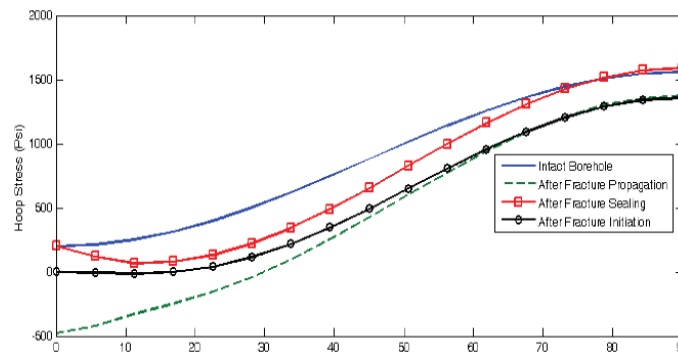

Figure A4: Hoop stress for WBS Alberty and Mclean (2004)

Salehi and Nygaard (20111) suggested the below shortcomings were behind the false results in the previous numerical simulations with respect to WS and estimation of fracture width:

- Fracture initiation was not simulated
- Propagation was not simulated
- Associated stress changes were not considered
- Poro-elastic rock parameters were Omitted
- Fracture permeability was not considered

Another criticism to the stress caging theory was raised by Van Oort, (2009). According to him, any increase in hoop stress should result in increase in the fracture initiation pressure (P_{ini}); based on Kirsch equation. However, this was not observed in any of the published date he revisited. Figure 5 is an idealized LOT for SC and FPR mechanisms.
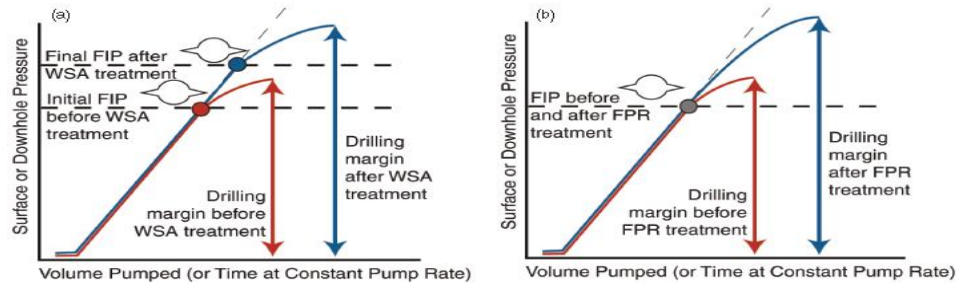

Figure A5: Idealized LOT for SC & FPR Van Oort, (2009).

It worth mentioning here that some lab experiment has shown an increase of P_{ini} while using Nano Partials (NPs) which was related to decrease fluid spurt loss/ penetration (Conteras et al., 2014).

Fracture Closure Stress.

Another WSA theory is the Fracture Closure Stress (FCS) introduced by Dupriest et al., (2005; 2008). The main principal is to increase the fracture closing stress (σ_h) by widening the fracture and propping it opened. Several numerical modeling studies were used to support this theory (Alberty and Mclean, 2004; Fuh et al., 1992).

The FCS is based on the net fracture pressure (NFP), which is derived from rock fracture mechanics and refer to the fracture pressure that exceeds the minimum far field stress, and it is in direct relation with the fracture length and width as shown in below equation:

$$P_{net} \propto \frac{E'}{R}\left(\mu q R / E'\right)^{1/4}$$

$$w \propto \left(\mu q R / E'\right)^{1/4}$$

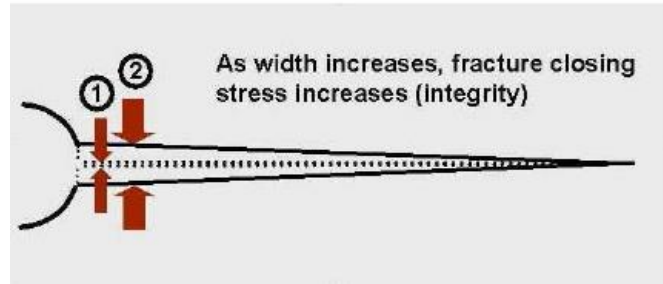So, the greater the NFP the greater the width would be. Figure 6 illustrate the concept.

Figure A6: FCS vs. Fracture width Dupriest et al., (2005)

However, once the fracture width reaches 100-200 microns, width to allow barite to enter the fracture, fracture propagation or LC would occur. Since the fracture tip acts as a relief valve, no further increase in fracture width could be obtained. Such a gain is mostly insufficient. Thus, in order to increase the closing stress, an additional increase in fracture width is required. This could be attained by blocking the fracture tip to the wellbore with LCM materials so wellbore pressure doesn't transmit to the tip. This is referred to as "Tip Resistance by the Development of an Immobile Mass". Nevertheless, if the width of LCM is inadequate to create sufficient closing stress, any increase in wellbore pressure would increase the fracture width. Therefore, causing the mud to bypass the blocking materials and leading to losses again. Figure 7 illustrates this concept where the well is static with no circulation but once ECD kicks in losses resumes.
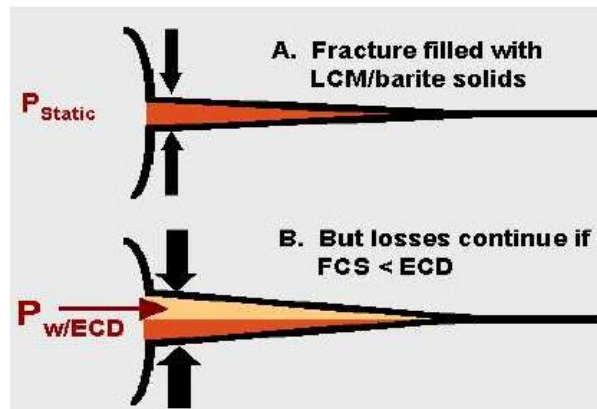

Figure A7: Inadequate closing Stress Dupriest et al., (2005)

One fracture width cannot be increased, with existing overbalance, the fracture will not be able to lengthen either. Thus, losses would be cured. Based on the above discussion, a successful treatment will require:

    I.   The blocking material must achieve and maintain isolation of fracture tip as fracture widens.

    II.   The final width must be sufficient to create a closing stress greater than ECD

Moreover, LCM is believed to isolate the fracture tip by forming an immobile mass. Due to the fluid loss to the formation matrix, carrier fluid dehydrates resulting in deposition of LCM.

However, in a low or damaged permeability environment such a technique is not functional. Thus, several developments have been done to enhance this process by either:

- Deposition of solids in layers via hesitation squeeze.
- Development of viscous resistance
- Deposition of adhesive solids.

Figure 8 summaries the FCS mechanism.

A. Fracture widens until it will accept barite-sized particles, then grows in length, but not width

B. Fluid loss creates immobile mass. Frac pressure increase as mass resists hydrostatic head. Pressure widens fracture.

C. Pressure is held. Filtrate loss continues unitl fracture is packed back to the wellbore. Width and increased FCS are trapped by solids.

D. In low permeability, or if great width is required, hesitaiton is conducted to build width in layers.
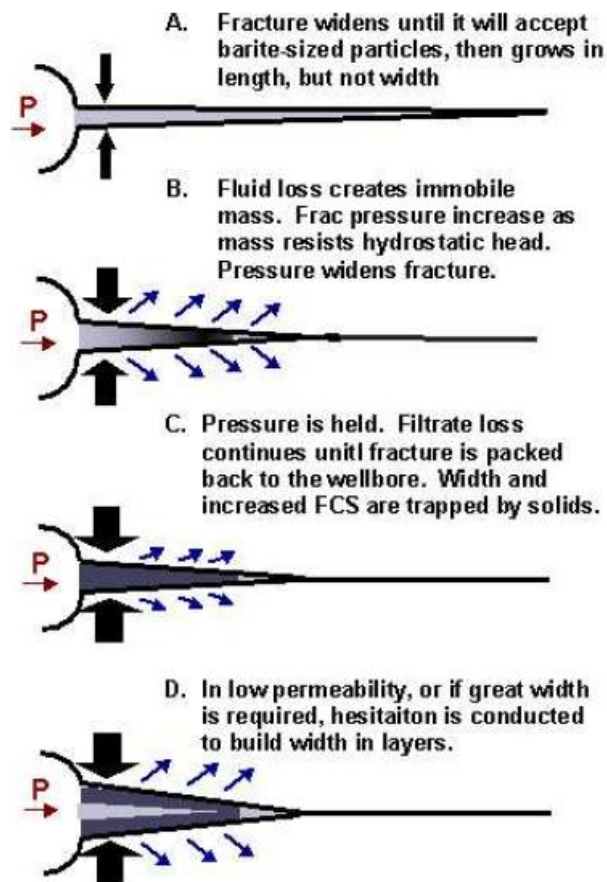
Figure A8: Inadequate closing Stress Dupriest et al., (2005)

In support of Alberty, Dupriest (2008) highlighted the importance of arresting the fracture growth early. He claimed that the success of a treatment is dependent of the length of the created fracture. Dupriest (2008) used a linear elastic finite element model to plot the propped fracture length vs. the required width, shown in Figure A9. The plot clearly shows that length and width of the fracture are in a direct relationship. Thus, a continuous treatment will either fail completely or achieve very small increased in FCS when fracture length is not constrained early.
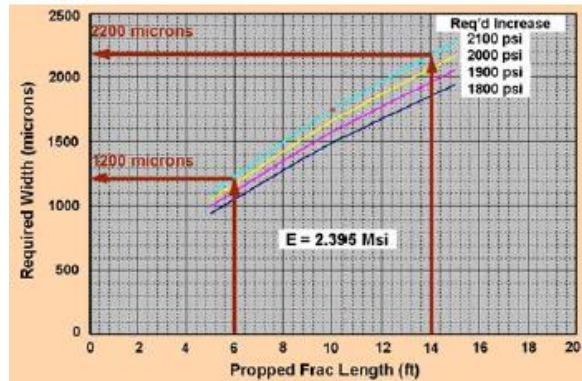

Figure A9: Length vs. Width FE model Dupriest (2008)

Due to the time consumption associated with applying FCS treatment, a preventative approach of this theory, Drill Stress Fluid (DSF) was introduced were the entire mud system in loaded with LCM prior to drilling the problematic zone. The DSF contains a high solids content with extremely high filtration rates; to prevent fracture tip extension (i.e. filtrate does not cause fracture extension) and thus eliminate fracture stress reduction. Figure A10 illustrates this concept. .
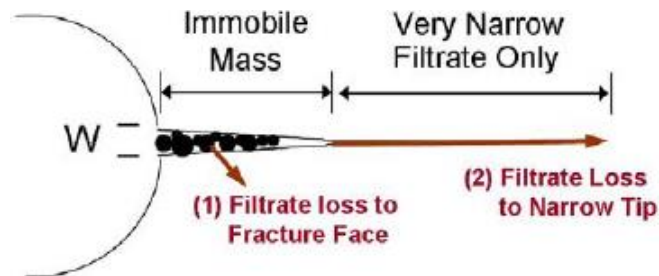

Figure A10: DSF process Dupriest (2008)

The designing criteria of the DSF were as follow:

- Maximizing Solids Content
- Maximizing Spurt Loss
- Minimize Packing Efficiency
- Particle Size and Fracture Geometry.

For more information about this fluid see (Dupriest et al., 2008).

The FCS approach has been criticized as well by some researchers. Salehi and Nygaard (20111), as an example, raises the same concerns regarding the poro elasticity model and the fracture inanition; explained in SC theroy. With respect to the reported increase in $P_{ini,}$ in FCS

application, Van Oort (2009) tied this observation to the difficulty in identifying the true P_{ini} in permeable formation. The fact that this approach was done in permeable formation where continuous fluid leaks off occurs could be the reason behind this apparent increase.

Fracture Propagation Resistance (FPR).

Fracture propagation resistance (FRP) concept was based on the foundation laid by DEA-13 and GPRI (Van Oort et al., 2009). The size of dehydrated mud zone behind the fracture tip, shown in Figure A11, found to be dependent on the amount of fluid loss and the fluid type; which explains why the WBM has higher P_{bd} than the O/SBM.
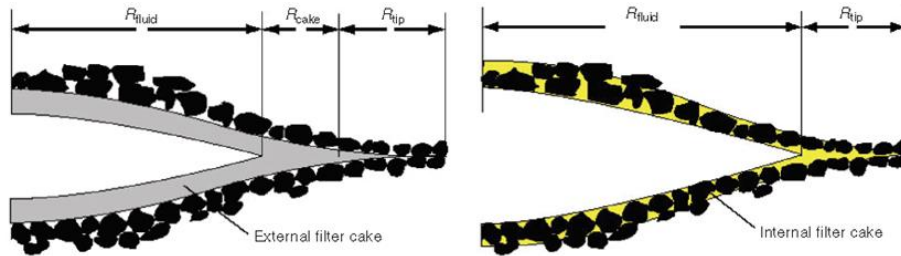

Figure A11: Close Look at Fractures with WBM & OBM (Van Oort et al., 2009).

Based on the results of DEA-13 Morita et al., (1990) came up with an analytical solution that predicts P_{bd}. Unlike the conventional method, the lost circulation pressure is not only dependent of tangential stress and tensile strength but it incorporates the following factors as well:

- Young's Modulus
- Borehole size
- Existing Crack size
- Width of closed fracture
- Type of drilling fluid.

In the favor of this theory, the experimental study by Fuh et al., (1992) showed that a specifically selected material based on strength, specific gravity, size distribution and concentration of granular material will successfully inhibit the initiation and propagation of the fractures while drilling. This is accomplished by plugging any small surface flows and isolating the tip of fracture "screen-out". Based on Fuh et al., (1992) for a successful FPR the below conditions must be met:

I. The concentration of particulate material should be increased with fracture propagation such that it packs around the fracture tip
II. The initial concentration of the particulate material is sufficiently high to induce screen-out while an induced fracture is still small
III. The packed particulate material should not allow drilling mud to leak through itself
IV. The packed particulate material has sufficient strength which can plug a sufficiently wide fracture tip region.

Likewise, Van Oort et al., (2009) built on this theory and used specifically designed WSMs in their approach. A laboratory evaluation of WSM performance and selection criteria for field operations were proposed.

Additional WS Mechanisms.

Several more mechanisms were introduced however with less popularity. Elastoplastic barrier model is an example of these mechanisms. This model was based on a 10-year research program of The University of Stavanger (Aadnoy et al., 2008; 2009). The research started on studying the deviation of the fracturing pressure vs. Kirsch approximation while using different fluids, Figure A12 shows this devation.
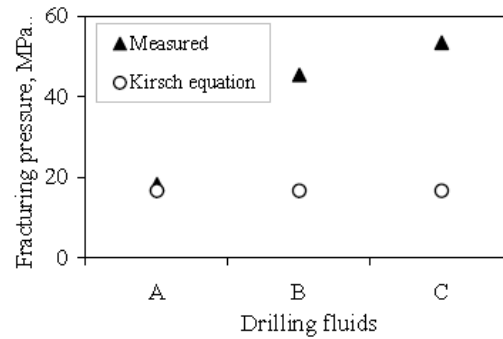

Figure A12: Theoretical Vs. Measured P_{bd} (Aadnoy et al., 2008)

This pressure deviation was linked to the stability of the filter cake. After analyzing the filter cake, it was found that it behaves plastically. Thus, the new model assumes a thin plastic layer of mud cake followed by a linearly elastic rock "elasto-plastic". The physical description is that when a fracture opens the mud cake doesn't split but it deforms plastically maintaining a barrier:

$$P_{bd} = 3S_h - S_H - P_0 + T_0 + \frac{2Y_0}{\sqrt{3}} \ln\left(1 + \frac{t}{r_w}\right)$$

Where t: barrier thickness,

Y_0: Barrier Partials' Yield Strength

The description of the fracturing process based on this mechanistic model is summarized in five phases shown in Table 2:
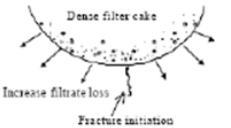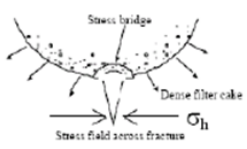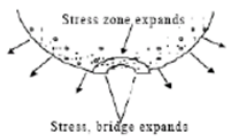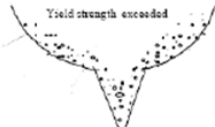
Event	Fig	Main controlling parameters
Filter cake formation		Filtrate loss
Fracture initiation		Filtrate loss, Stress
Fracture growth		Bridge stress Rock stress
Further fracture growth		Bridge/rock stress Particle strength
Filter cake collapse		Particle strength

Table A2: Elasto-Plastic Model (Aadnoy et al., 2008)

For more information, refer to the mentioned papers.

Another theory is the wellbore Shielding by utilizing Fast-Sealing LCM (FS-LCM) (Wang et al., 2016). The theory evolves around the concept of spurt losses. In order to stop an induced fracture from creating a seal is formed after only a small volume flows into the fracture. Rock properties along with anticipated pressure and largest particlesize are used to estimate the allowed fluid spurt loss for the system.
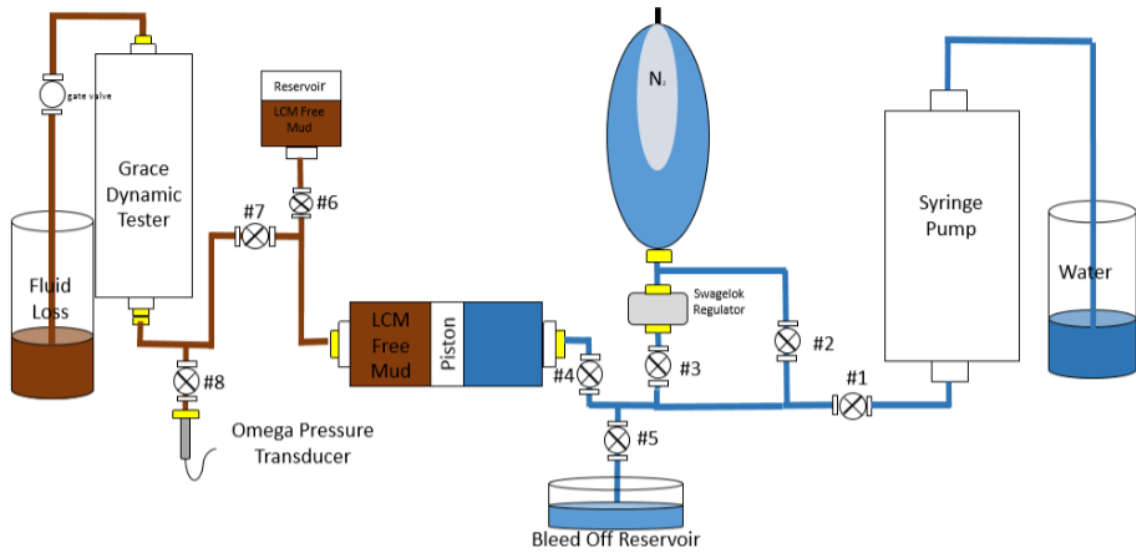
B. TESTING PROCEDURE

Figure B1: Apparatus layout

Filling up the bladder accumulator:

1. Valves number 1 and 2 have to be in open position.

2. All other valves have to be in closed position.

3. Start the pump at 20 ml/min and set the maximum pressure at 3800 psi.

4. Monitor the pressure through both pump and regulator gauge.

5. Once pump pressure reading reached 3800 psi, pumping should be concluded and the bladder accumulator should be ready to be used.

6. Close Valve number 2 and open Valve number 5 to bleed off remaining pressure.

Filling up floating piston accumulator with Mud:

1. Valves number 4, 5 and 6 have to be in open position.

2. All other valves need to be closed.

3. Open up the cap on the plastic accumulator and fill it with mud to the top and then close the cap.

4. Connect the air hose to the top of the plastic accumulator and start applying air pressure to displace the drilling fluid. Bleed off reservoir filling should be noticed during the displacement operation.

5. Repeat step #4 until no further mud can be displaced.

Note: Bleed off air pressure from air compressor bleed off valve prior to open the plastic accumulator cap.

Dynamic Fluid Loss test with constant flow rate:

1. Valves number 1, 4, 7 & 8 have to be in open position.

2. All other valves need to be closed.

3. Fil up the testing cell with LCM Mud to below the disc.

4. Insert the disc and Fill up the rest with LCM Free mud.

5. Connect the cap and place the cell into the grace cradle.

6. Connect the flow out assembly.

7. Connect the Swagelok tube connection to the bottom of Grace dynamic cell, make sure to back out the stem valve ½ turn prior to connection.

8. Connect the shaft to the paddle assembly.

9. The cell is now ready for testing.

10. Open up the gate valve at the flow out and start pumping.

11. Once test is done and the pump is switch off, open valve # 5 to bleed off any trap pressure.

Dynamic Fluid Loss test with constant pressure:

1. Valves number 1, 3, 4, 7 & 8 are needed to be in opened position.

2. All other valves need to be closed.

3. Fil up the testing cell with LCM Mud to below the disc.

4. Insert the disc and Fill up the rest with LCM Free mud.

5. Connect the cap and place the cell into the grace cradle.

6. Connect the flow out assembly.

7. Connect the Swagelok tube connection to the bottom of Grace dynamic cell, make sure to back out the stem valve ½ turn prior to connection.

8. Connect the shaft to the paddle assembly.

9. The cell is now ready for testing.

10. Adjust the required pre-pressure from the Swagelok regulator and open up gate valve at the flow out.

11. Once test is done and the regulator valve is closed, open valve # 5 to bleed off any trap pressure.

VITA

Ghassan Dhiya Alshubbar

Candidate for the Degree of

Master of Science

Thesis: EVALUATION OF CONVENTIOANL LCM TREATMENTS IN
FRACTURED AND VUGGY FORMATIONS.

Major Field: Petroleum Engineering

Biographical:

Education:

Completed the requirements for the Master of Science in Petroleum Engineering
at Oklahoma State University, Stillwater, Oklahoma in December, 2017.

Completed the requirements for the Bachelor of Science Petroleum and Natural
Gas Engineering at West Virginia University, Morgantown, WV, US in 2010.

Experience: Wellsite Supervisor at Saudi Aramco since 2012.